grown in 6-well plates to nearly 100% confluency were infected with a diluted whole-cell extract of HSV-2(G)-infected cells. The whole cell extract was prepared by three repeats of freeze-thaw disruption of HSV-2(G)-infected cells. After 1 h adsorption, the inoculum was removed and the cell monolayer was overlaid with Dulbecco's modified Eagle medium (DMEM) containing 1% fetal calf serum (FCS) and 0.16 mg/ml pooled human immunoglobulin (Sigma). The overlaid medium was removed after 2 days of infection, and the infected cell monolayer was fixed and stained with methanol and 0.1% crystal violet, respectively.

Confocal immunofluorescence microscopy

Twenty-four hours after the transfection, cells on 15-mm glass coverslips were fixed with 4% paraformaldehyde for 10 min, permeabilized with 0.5% Triton X-100 for 20 min, blocked with the blocking solution (0.2% Gelatin, 1% BSA, 0.05% Tween 20 in PBS) for 30 min and reacted with a diluted primary antibody in the blocking solution for 12 h at 4°C. After incubation, cells were washed extensively with a washing solution [0.05% Tween 20 in PBS (pH 8.0)], incubated for 2 h at room temperature with the appropriate secondary antibody diluted in the blocking solution, and then washed three times with the washing solution. The cells were analyzed under a confocal microscope (Olympus; FV1000; confocal aperture, 300 μm) through a PLAPO 60× NA:1.40 objective lens. ICP27 and PML-NB signals were collected sequentially by excitation with a 488 nm laser and a 543 nm laser, respectively.

Transfection of plasmids and siRNAs

HeLa, HEK293, and Vero cells were grown in DMEM (Nacalai) supplemented with 10% heat-inactivated FCS, and then maintained by the standard protocol. HeLa and HEK293 cells were transfected with GeneJuice (Roche) or Lipofectamine 2000 (Invitrogen) and TransIT293 (Mirus), respectively. All plasmids used for transfection were prepared using a Maxiprep kit (Biogene). HEK293 cells were grown in a monolayer in 6-well plates, and then co-transfected with 500 ng per well of a reporter plasmid and 500 ng of either myc-vector or plasmids expressing myc-tagged HSV-2 proteins.

siRNA transfection was performed in 12-well plates by transfecting HeLa cells with 20 pmol per well of siRNAs against either the *LacZ* reporter (Invitrogen) or *PML* (Invitrogen, UCUUGGAUACAGCUGCAUCUUUC CC), using Lipofectamine RNAiMAX (Invitrogen).

In vitro splicing reaction

The PCR products of human T7-PML wt (exon 7, 53 nt; intron 7a, 641 nt; and exon 7b, 213 nt) and T7-PML d1 (exon 7, 53 nt; intron 7a, 257 nt; and exon 7b, 213 nt) were used as the DNA template for T7 transcription. Pre-mRNA substrates were m7GpppG-capped and ^{32}P-labeled by *in vitro* transcription. *In vitro* splicing reactions were performed in 20 μl volumes at 30°C under the conditions described by Krainer *et al.* (40). As shown in Figure 6E, highly purified Flag-ICP27 was added in the reaction system. After the reaction, RNA was subjected to denaturing PAGE analysis and autoradiography.

RNA immunoprecipitation

Nuclear extracts were prepared from HEK293 cells transfected with plasmids expressing Flag alone, Flag-ICP27 wild-type and M15. ^{32}P-labeled PML exon 7-7b, β-globin and δ-crystallin RNA were prepared by *in vitro* transcription with [α-^{32}P]UTP and T7 RNA polymerase (Takara). Gel purified RNA was incubated for 30 min at 30°C with each nuclear extract in 20 μl of RNA binding buffer [20 mM HEPES–KOH (pH 7.9), 100 mM KCl, 5% Glycerol, 1% Triton X-100, 2 mM DTT and 0.2 mM PMSF] supplemented with 0.4 U of an RNase inhibitor (Promega), and immunoprecipitation was then performed with Flag-M2 antibody. Each RNA was purified by the protein removal and ethanol precipitation. The purified RNAs were analyzed by denaturing PAGE and imaging using a phosphoimage analyzer (FLA-3000G; FUJIFILM).

Preparation of stable transfected T-REx293 cells

T-REx293 cells (the HEK293 cell line expressing a tetracycline repressor obtained from Invitrogen) were grown following the manufacturer's protocol in DMEM (Nacalai) containing 10% heat-inactivated FCS and 10 mg/ml blasticidin (Invitrogen). To generate stably transfected tetracycline inducible cell lines, T-REx293 cells were co-transfected with either pcDNA5-Flag or pcDNA5-Flag-ICP27. After 48 h post-transfection, these transfected cells were grown in the presence of 0.1 mg/ml hygromycin B following the manufacturer's protocol to select stable transfected clones.

RESULTS

HSV-2 infection switches the expression pattern of PML isoforms

We first compared the splicing patterns of PML transcripts from HeLa cells, with and without HSV-2 infection. Total RNAs of HeLa cells were collected immediately (0 h post-infection, 0 hpi) and 3 h post-infection (3 hpi). The RT–PCR analysis, using the primer sets indicated in Figure 1A, showed that the amounts of mRNAs containing PML-I-specific exon 8-9 and PML-II-specific exon 6-7b were reduced in the HSV-2-infected HeLa cells (Supplementary Figure S1A and Figure 1B, top, lane 4), whereas the amounts of PML mRNA containing constitutive exon 1-4 (Supplementary Figure S1A) and exon 6-7 (Figure 1B. middle, lane 4), and GAPDH mRNA were much less reduced (Figure 1B, bottom, lane 4 and Supplementary Figure S1A).

Moreover, we examined other cellular mRNAs containing constitutive introns (Aly/REF intron 4, Lamin A/C intron 6), alternative introns (Lamin A/C introns 9 and 10) and minor introns (P120 intron 6, HPS1 intron 16) by RT–PCR analysis. The expression levels and splicing patterns of the mRNAs containing these introns were not significantly changed (Supplementary

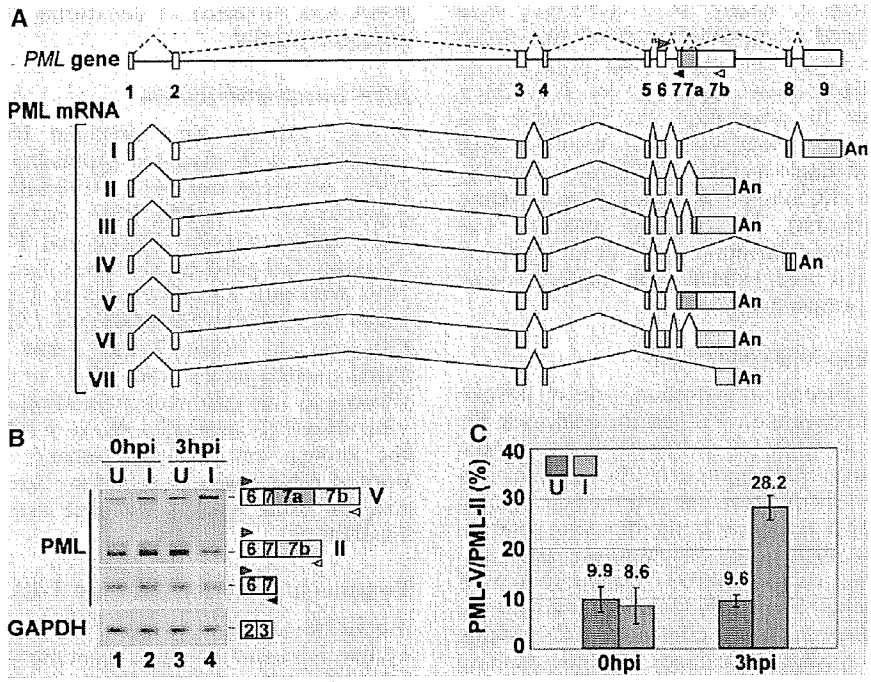

Figure 1. Modulation of PML expression by HSV-2 infection. (**A**) Schematic representation of the *PML* gene and mRNA species generated by alternative splicing. The positions of different primer sets used for RT-PCR are indicated by colored arrow heads. (**B**) RT–PCR analysis (28 cycles) of uninfected (U: lanes 1 and 3) and HSV-2-infected (I: lanes 2 and 4) HeLa cells at MOI 1 (0 hpi and 3 hpi). GAPDH primers were used as a control. (**C**) Graphic representation of the splicing ratios PML-V/PML-II. Green and red box indicate the splicing ratio in HSV-2-infected (I) and uninfected (U) cells, respectively ($n = 3$).

Figure S1B). Interestingly, the amount of mRNA containing PML-V-specific exon 7-7a-7b was increased in the HSV-2-infected cells (Figure 1B, top). The quantitative analysis also showed that the ratio of PML splicing isoforms (PML-V/PML-II) was enhanced by HSV-2 infection (Figure 1C, 2.9-fold in 3 hpi). Consistent with the reduction in PML-II-specific exon 7-7b, PML-II foci recognized by PML-II-specific antibody were reduced in the HSV-2-infected cells (Supplementary Figure S2). These observations indicate that HSV-2 infection changes the alternative splicing of PML pre-mRNA.

The splicing reporter of PML gene is sensitive to HSV-2 infection

We have recently succeeded in visualizing the tissue-specific regulation of alternative pre-mRNA splicing in live nematodes by developing a transgenic reporter system with fluorescent proteins (35). Using this system, we have identified three genes as alternative splicing regulators (35,36). To clarify the HSV-2-mediated regulatory mechanism of alternative splicing of the PML pre-mRNA, we prepared splicing reporter minigene constructs containing the region from exon 6 to exon 7b of the PML gene without or with the red fluorescent protein (RFP) coding region, and named them E6-7b and E6-7b-RFP, respectively (Figure 2A). The splicing reporter E6-7b-RFP can express RFP only when intron 7a is spliced out and the PML-II form is produced. Notably, when we transfected E6-7b-RFP into HeLa cells, RFP was detected in the transfected cells. To examine whether or not we can use E6-7b-RFP as a screening tool of viral splicing regulators, we observed RFP expression in Venus-HSV-2-infected cells. As we initially assumed, the RFP expression was reduced in the Venus-HSV-2-infected cells in a viral titer-dependent manner (Figure 2B and Supplementary Figure S3), suggesting that the minigene reporter reflects the splicing alteration induced by HSV-2 infection. To examine whether or not the reduction of RFP expression was caused by HSV-2 regulated-pre-mRNA splicing, we performed RT–PCR analysis of HeLa cells transfected with the E6-7b (Figure 2C, lanes 1 and 2) or E6-7b-RFP (Figure 2C, lanes 3 and 4) reporter and then infected with HSV-2 at MOI 10 for 3 hours (Figure 2C, lanes 2 and 4). Regardless of the additional RFP coding region, the promotion of intron 7a retention in the HSV-2-infected HEK293 cells was confirmed by RT–PCR (Figure 2C, lanes 3 and 4). The incomplete retention of intron 7a by HSV-2 infection might be caused by the remaining uninfected cells under the experimental condition, as shown in Figure 1B, lanes 4. These observations indicate that the E6-7b-RFP reporter can be used as a screening tool of viral splicing regulators.

The viral protein ICP27 switches the splicing pattern of PML pre-mRNA

To identify viral splicing regulator(s), HSV-2 cDNAs coding 26 viral nuclear proteins of HSV-2 were co-transfected with PML E6-7b-RFP into HeLa cells,

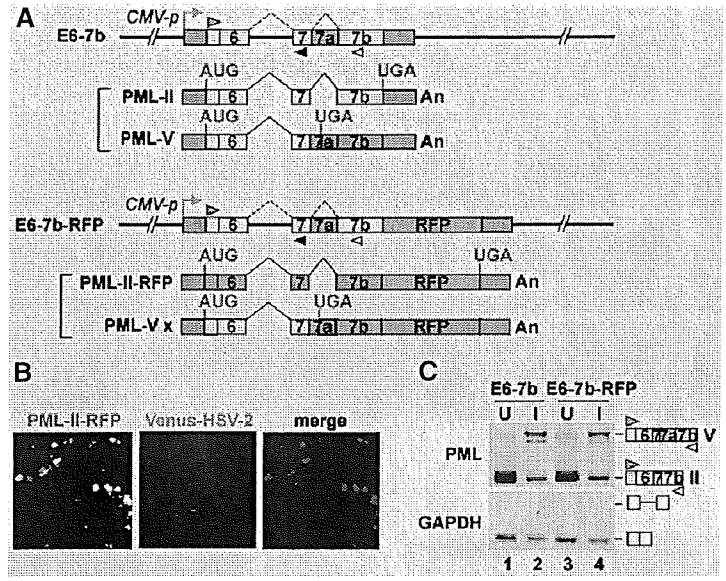

Figure 2. Visualization of virus-sensitive splicing reporter of the *PML* gene. (**A**) Schematic representation of two splicing reporters. The splicing reporter involving the *PML* gene from exon 6 to exon 7b with (E6-7b-RFP) or without (E6-7b) the RFP coding region, and mRNAs derived from the reporter. Predicted ORFs are indicated in red (PML-II-RFP) or gray (PML-V x), and UTRs in dark gray. The positions of different primer sets used for RT–PCR are indicated. This reporter is driven by the CMV promoter. (**B**) Microscopy analysis of Venus-HSV-2-infected cells. HeLa cells were infected with Venus-HSV-2 at MOI 0.01. After 3 h infection, E6-7b-RFP was transfected into the cells. After 24 h infection, RFP expression was reduced particularly in Venus-HSV-2 infected cells, although RFP was well detected in uninfected cells. Venus-HSV-2 is indicated in green. (**C**) RT–PCR analysis of uninfected (U) and infected (I) HeLa cells at MOI 10 (3 hpi), into which either E6-7b or E6-7b-RFP constructs were transfected.

and it was demonstrated that RFP expression was lost only in the cells transfected with the ICP27 or UL41 expression vector (Figure 3A, panels 3 and 22). Furthermore, the reduction of RFP expression was also checked by western blot (Supplementary Figure S4). ICP27 overexpression dramatically switched the mRNA expression pattern of the PML E6-7b reporter from the PML-II-specific exon 7-7b form to the PML-V-specific exon 7-7a-7b form (Figure 3B, top, lane 3), whereas other viral nuclear proteins such as ICP22 or ICP0 did not affect the splicing (Figure 3B, top, lanes 4 and 5). Also, the amounts of expressed viral proteins were almost the same (Figure 3B, bottom). In contrast to ICP27, the overexpression of UL41 encoding a viral nuclease (41) suppressed PML-II-RFP expression owing to the promotion of PML-II-RFP RNA degradation (data not shown). To investigate whether ICP27 can induce switching of the endogenous PML splicing isoform, we transfected myc-tagged ICP27 cDNA and then checked for endogenous PML transcripts by RT–PCR analysis using a combination of exon 6-forward and exon 7b-reverse primers. The results showed that the intron 7a retention of endogenous PML transcripts was promoted in proportion to the amount of transfected ICP27 cDNA (Figure 3C, top and bottom); however, ICP27 did not inhibit the removal of other introns in PML pre-mRNA (Figure 3C, upper middle) or actin pre-mRNA (Figure 3C, lower middle). The foci in myc-tagged ICP27-expressing cells that were recognized by anti-PML-II antibody were decreased (Figure 3D, center), whereas those recognized by anti-PML-V sera were increased (Figure 3D, right) compared with untransfected HeLa cells. Moreover, the endogenous PML-II mRNA was switched to PML-V mRNA in a Flag-tagged ICP27 stable expressing cell line (T-REx293/Flag-ICP27), whose transcription was regulated by tetracycline addition (Figure 3E). However, as far as we have checked, the removal of the other introns containing the constitutive introns, alternative intron and minor introns was not affected by Flag-ICP27 (Supplementary Figure S1C). These observations indicate that ICP27 preferentially switches the expression of PML isoforms from PML-II to PML-V.

Interestingly, the foci recognized by anti-Pan-PML antibody were unchanged or only slightly decreased (Figure 3D, left). Although PML-I-specific exon 8-9 transcripts were decreased in HSV-2-infected cells, they were not changed in ICP27-expressing cells (Supplementary Figure S1A). These results suggest that PML-I mRNA expression is regulated by other viral factors other than ICP27 or cellular signal induced proteins (e.g. interferon stimulating factors) in HSV-2-infected cells.

KH3 domain of ICP27 is required to switch the PML isoform

As shown in Figure 4A, ICP27 contains defined functional domains, including a nuclear export signal (NES), the arginine- and glycine-rich motif (RGG box), the

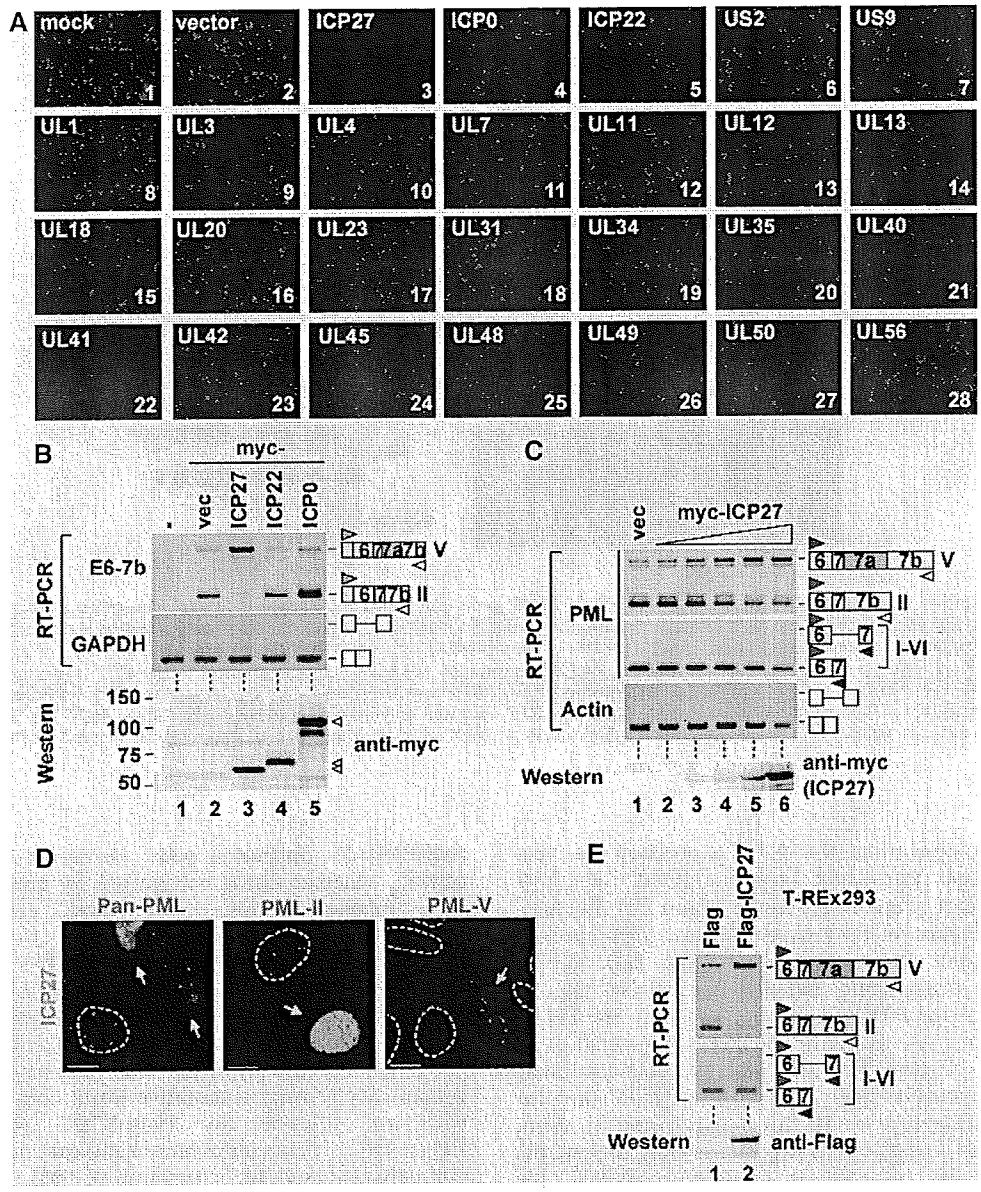

Figure 3. Retention of PML intron 7a by ICP27. (A) Microscopy analysis of HeLa cells transfected with the combinations of the E6-7b-RFP construct and each HSV-2 cDNA performed by detecting RFP signaling (red). DNAs were stained with DAPI (blue). (B) RT–PCR analysis of HEK293 cells transfected with the combinations of E6-7b constructs and plasmids containing myc-tagged HSV-2 cDNA (B, upper panels). Whole-cell extracts of HEK293 cells transfected with these plasmids were subjected to western blot analysis for myc-tag (B, bottom). (C) RT–PCR, using the primers shown in Figure 1A, and western blot analysis of HEK293 cells transfected with 2-fold dilution series of myc-tagged ICP27. (D) Immunofluorescence of HeLa cells transfected with myc-tagged ICP27. PML-NBs were stained with anti-Pan-PML (left), PML-II specific (center) and PML-V specific (right) sera. Scale bar, 10 μm. Yellow arrows indicate ICP27-transfected cells. (E) RT–PCR analysis, using the primers shown in Figure 1A, and western blot analysis for Flag-tag of T-REx293 expressing Flag-tag peptides and Flag-ICP27.

RGG box with nearby sequence (R2) and 3 KH domains. To identify the ICP27 region required to promote retention of intron 7a of PML, we prepared a series of ICP27 mutants lacking NES (d1-2), the RGG box (ΔRGG), and the RGG box plus R2 (ΔRR2) (Figure 4A). Overexpression of the deletion mutants of ICP27 retained the promotion activity for intron 7a retention (Figure 4B, top, lanes 4–6), whereas ICP27 mutant M15 containing altered residues at 465 and 466 (P465L/G466E) in the KH3 domain (42) failed to switch the alternative splicing of PML pre-mRNA (Figure 4B, top, lane 7). Wild-type ICP27 and the mutants were equally expressed in individual transfected cells (Figure 4B, bottom), and the foci of PML-II were unaffected by M15 expression (Figure 4C,

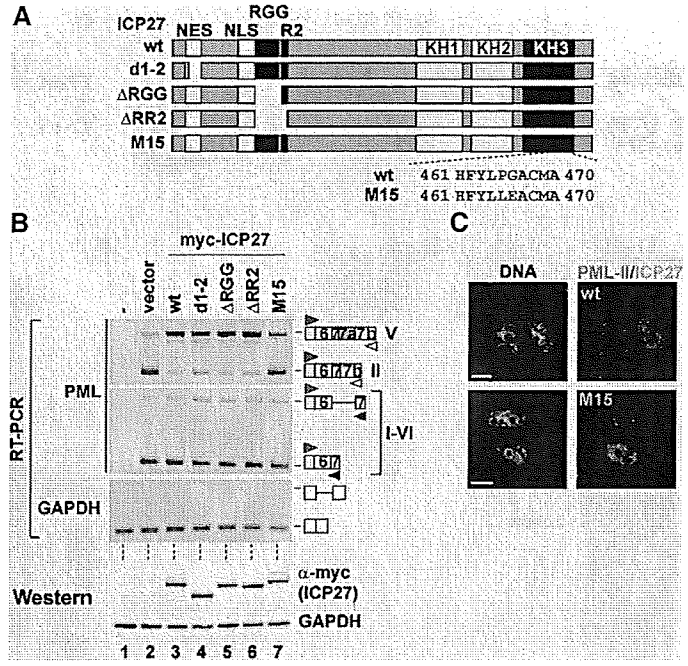

Figure 4. Effects of ICP27 mutants on PML RNA splicing. (A) Schematic representation of the structure of ICP27 mutants. (B) RT–PCR and western blot analysis of HEK293 cells transfected with either myc-tagged ICP27 wild-type or mutant plasmids. (C) Immunofluorescence of HeLa cells transfected with either myc-tagged ICP27 wild-type or the M15 plasmid, stained with anti-myc antibody and PML-II specific sera.

lower panels). These results indicate that the KH3 domain of ICP27 is critical for the switching of the PML isoform from PML-II to PML-V.

Since the ICP27 protein of HSV-1 is highly homologous to that of HSV-2, which we used, we next tested whether HSV-1 ICP27 protein could also affect the PML splicing or not. The ICP27 of HSV-1 also promoted the intron retention of PML splicing (Supplementary Figure S5A, lane 4). The *ICP27* gene is conserved in all members of the herpesvirus family. The *UL69* gene (cytomegalovirus; CMV), *EB2* (or *SM*) gene (Epstein–Barr virus; EBV) and *ORF57* gene (Kaposi's sarcoma-associated herpesvirus; KSHV and the herpesvirus saimiri; HVS) are homologues of the *ICP27* gene of each virus. In addition, the amino acids PG at 465 and 466 in the KH3 domain of ICP27, which are essential for splicing regulation of PML pre-mRNA (Figure 4B), are conserved within herpesviridae (Supplementary Figure S5B) (43). Furthermore, ICP27 and ORF57 reportedly promote intron retention of viral RNA (44,45). Taken together, these observations strongly suggest that ICP27-mediated alternative splicing of PML pre-mRNA is a common feature in the herpesvirus family.

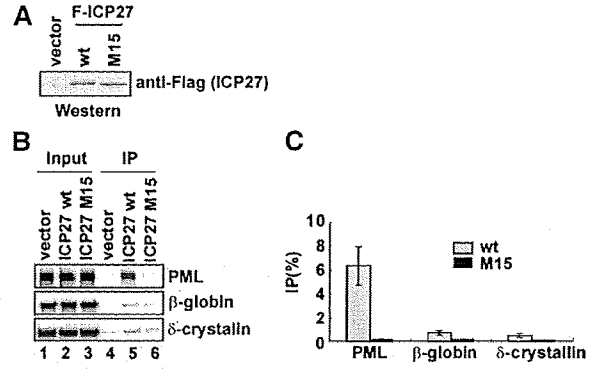

Figure 5. RNA binding specificity of ICP27. (A) Western blot analysis, using anti-Flag antibody, of nuclear extract from HEK293 cells transfected with Flag-vector and Flag-ICP27 wild-type (wt) and M15 expression plasmids. (B) RNA immunoprecipitation. Each ^{32}P-labeled *in vitro* transcript was incubated with the nuclear extracts from HEK293 cells expressing Flag-tag or Flag-tagged ICP27, and then immunoprecipitated with anti-Flag antibody. (C) Quantitation of three independent experiments is shown. Error bars represent SDs ($n = 3$).

ICP27 is specifically associated with PML pre-mRNA

To examine whether or not ICP27 preferentially associates with PML pre-mRNA, we performed RNA immunoprecipitation assay. Three pre-mRNAs containing human PML exon 7 to exon 7b, human β-globin exon 1 to exon 2 and chicken δ-crystallin exon 14 to exon 15, which were synthesized by *in vitro* transcription and labeled with [α-^{32}P] UTP, were mixed with the nuclear extract from HEK293 cells expressing Flag-tagged ICP27 (Figure 5A). Following incubation, RNAs were immunoprecipitated with anti-Flag antibody. The results showed that Flag-ICP27 was co-immunoprecipitated with PML pre-mRNA more efficiently (9.3- to 14.0-fold) than β-globin and δ-crystallin pre-mRNAs (Figure 5B, lane 5

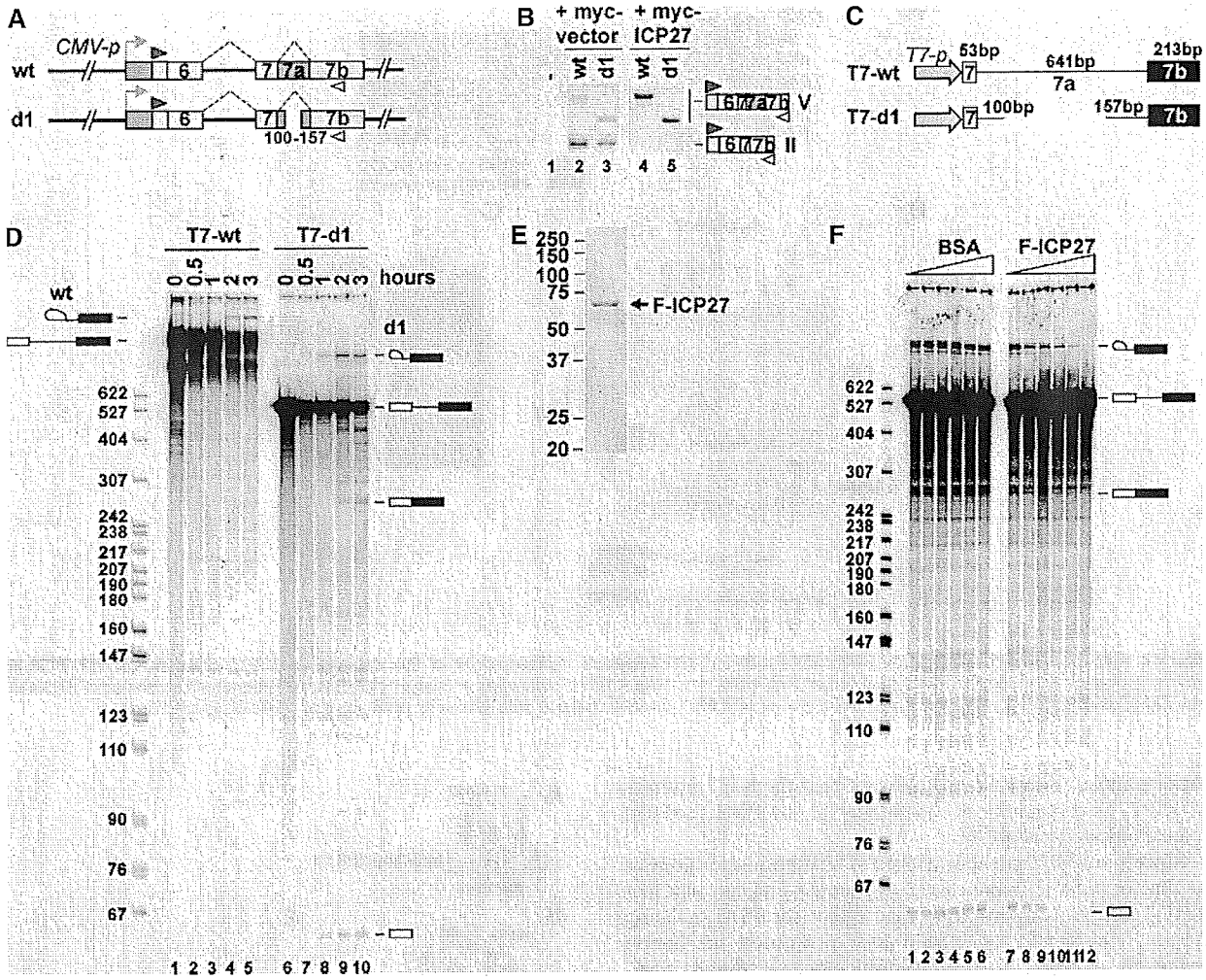

Figure 6. Inhibition of PML pre-mRNA splicing by ICP27. **(A)** Schematic representation of E6-7b wt and deletion-mutant splicing reporters, d1. The reporter E6-7b d1 contains a 100-bp fragment downstream of the 5′ ss and a 157-bp fragment upstream of the 3′ ss of intron 7a. **(B)** RT–PCR analysis of HEK293 cells transfected with Flag-vector (lane 1), and the combination of either E6-7b wt (lanes 2 and 4) or d1 (lanes 3 and 5) with either myc-vector (lanes 2 and 3) or myc-ICP27 (lanes 4 and 5). **(C)** Schematic representation of three E7-7b DNA templates, T7-wt (exon 7: 53 bp; intron 7a: 641 bp; exon 7b: 213 bp) and T7-d1 (exon 7: 53 bp; intron 7a: 257 bp; exon 7b: 213 bp), which are driven by the T7 promoter. **(D)** *In vitro* splicing of T7-wt (lanes 1–5) and T7-d1 (lanes 6–10) for the indicated time. The size of the pBR322 MspI-digested DNA marker is indicated on the right side of the panel. The pre-mRNA, mature mRNA and splicing intermediates are described on both sides of the panel. **(E)** A 10% SDS–PAGE and CBB staining of the purified Flag-ICP27 from the nuclear extract of T-Rex 293 cells expressing Flag-ICP27. **(F)** Effects of ICP27 on T7-d1 splicing *in vitro*. Two-fold dilution series (0, 25, 50, 100, 200 and 400 ng) of BSA (lanes 1–6) and highly purified Flag-ICP27 (lanes 7–12) were added to the *in vitro* splicing reaction.

and 5C, gray bars). Further, RNA immunoprecipitation experiment using the nuclear extract from HEK293 cells expressing Flag-ICP27 mutant M15 demonstrated that Flag-ICP27 mutant M15 was not co-immunoprecipitated with these pre-mRNAs (Figure 5B, lane 6 and 5C, black bars). Moreover, the amounts of Flag-ICP27 wild-type and M15 proteins were almost equally expressed (Figure 5A), indicating that ICP27 specifically associated with PML pre-mRNA, at least among cellular pre-mRNAs, and that the associations depended on the KH domains, which were presumably the RNA binding sites.

ICP27 directly inhibits the removal of PML intron 7a

To examine whether or not ICP27 directly inhibits PML pre-mRNA splicing, we performed an *in vitro* splicing reaction. The DNA template T7-wt containing a T7 promoter and PML exon 7 to exon 7b was prepared by PCR and used for T7 transcription (Figure 6C). The *in vitro* splicing reaction resulted in the T7-wt transcript slightly generating splicing intermediates (Figure 6D, lanes 1–5), which led us to modify the T7-wt DNA template. We prepared the mutant d1 which has deletion in intron 7a, as described in Figure 6A. Transfection of the d1 construct showed that the PML d1 transcript was efficiently

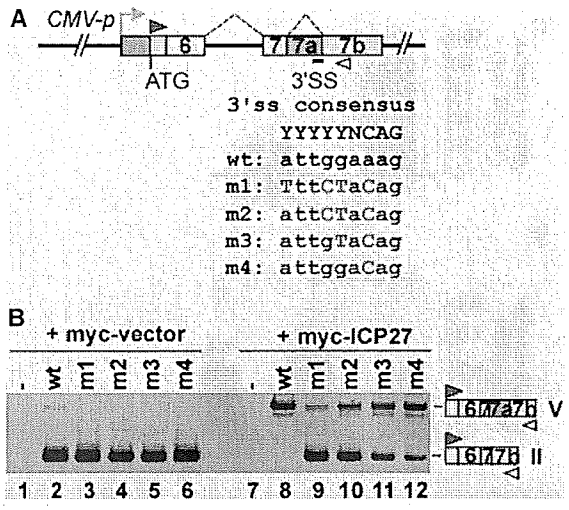

Figure 7. The weak 3′ ss essential for ICP27-mediated alternative splicing of PML pre-mRNA. (**A**) Scheme of the E6-7b construct wild-type and a series of point mutations at the 3′ ss in PML intron 7a. (**B**) Results of RT–PCR analysis of HeLa cells transfected with each E6-7b *cis*-mutant and myc-tagged ICP27.

removed from intron 7a and that intron 7a of d1 RNA was retained by myc-ICP27, as well as the PML wt transcript (Figure 6B, lanes 3 and 5). These results indicate that the PML d1 mutant can be useful for *in vitro* splicing reactions. The *in vitro* splicing of the T7-d1 transcript showed that it was more efficiently spliced than the T7-wt transcript (Figure 6D, lanes 6–10). Next, we examined the effects of ICP27 on PML splicing. Flag-ICP27 was purified from T-REx293 cells expressing Flag-ICP27, and then the highly purified Flag-ICP27 was added to the *in vitro* splicing reaction using d1 mutant RNA. The results showed that the productions of T7-d1 spliced mRNA and intermediates were inhibited by the addition of purified Flag-ICP27 in a dose-dependent manner (Figure 6F, lanes 7–12), but not by BSA (Figure 6F, lanes 1–6). These results indicate that ICP27 directly inhibits PML pre-mRNA splicing.

3′ Splice site of intron 7a of PML pre-mRNA is critical for ICP27-mediated switching

The alternative splicing depends on the utilization of the 5′ ss and 3′ ss at the end of introns (3). The 5′ ss includes a GU dinucleotide at the intron end encompassed within a less conserved consensus sequence. At the other end of the intron, the 3′ ss region has conserved a polypyrimidine tract capable of associating with U2AF65/35, followed by a terminal AG at the extreme 3′-end of the intron (YYYYYNCAG) (46). In contrast, the 3′ ss sequence of PML intron 7a is a purine-rich sequence (ATTGGAA AG). To evaluate the involvement of the atypical 3′ ss of intron 7a for the ICP27-mediated switching from PML-II to PML-V, we mutated the 3′ ss region of intron 7a in the PML E6-7b reporter to match with the 3′ ss consensus sequence (Figure 7A, m1-m4). RT–PCR analysis showed that the ICP27-induced retention of PML intron 7a was diminished in proportion to the number of mutated nucleotides at the 3′ ss (Figure 7B, lanes 8–12).

PML splicing isoform II contributes to production of infectious HSV-2

To examine the differential roles of PML isoforms in host-virus interactions, we attempted rescue experiments with a siRNA-resistant PML isoform in PML pre-knocked down HeLa cells. We first efficiently knocked down all PML isoforms from HeLa cells with siRNA (siPML4) against PML exon 4. Following 48 h of siRNA transfection, HSV-2 was infected and then HSV-2 titer was measured by plaque assay (Figure 8A). siPML4 efficiently knocked down endogenous PML isoforms (Figure 8B, lane 2), whereas control siRNA (siLacZ) did not knock down any of them (Figure 8B, lane 1). Plaque assay revealed that HSV-2 replication was suppressed by ~80% in the PML-knocked-down HeLa cells (Figure 8C), consistent with the results of the immunofluorescence analysis (Supplementary Figure S6). We then transfected these cells with a plasmid encoding either RFP, RFP-PML-II or RFP-PML-V with a silent mutation that makes the PML isoform resistant to siPML4, and thereafter evaluated the plaque-forming activity of the virus (Figure 8D). The rescue experiment showed that RFP-PML-II increased the HSV-2 plaque number (~1.6-fold RFP), but RFP-PML-V did not (Figure 8F), although the expression levels of the RFP-PML-II and RFP-PML-V mRNAs were similar (Figure 8E, lanes 2 and 3). The result showed that the difference in the rescue experiments between only RFP and RFP-PML-II appeared smaller than the reduction of HSV-2 replication by the knock-down of all PML isoforms. One possible explanation is the transfection efficiencies of RFP (43%), RFP-PML-II (33%) and RFP-PML-V (34%) (Supplementary Figure S7). These observations suggest that the difference in HSV-2 plaque number may become larger if all cells expressed siRNA-resistant PML isoforms, suggesting that PML-II plays a specific role in efficient HSV-2 replication.

DISCUSSION

In this study, we identified *ICP27* as a splicing regulator of PML pre-mRNA, showing the possibility that the viral protein switches alternative splicing of specific cellular RNA in association with functional alteration.

Selective splicing regulation by ICP27

HSV ICP27 is one of the immediate early (IE) proteins of HSV and plays an essential role in the expression of viral late genes (47,48). ICP27 interacts and co-localizes with cellular splicing factors, such as small nuclear ribonucleoproteins (snRNPs) (49), SR proteins, SR protein kinase 1 (SRPK1) (50) and spliceosome-associated protein 145 (SAP145) (51), and is suggested to inhibit the splicing of cellular pre-mRNAs by impairing spliceosomal assembly (50). However, considering that some essential viral pre-mRNAs such as ICP0 have introns and require splicing, it is less likely that HSV suppresses constitutive

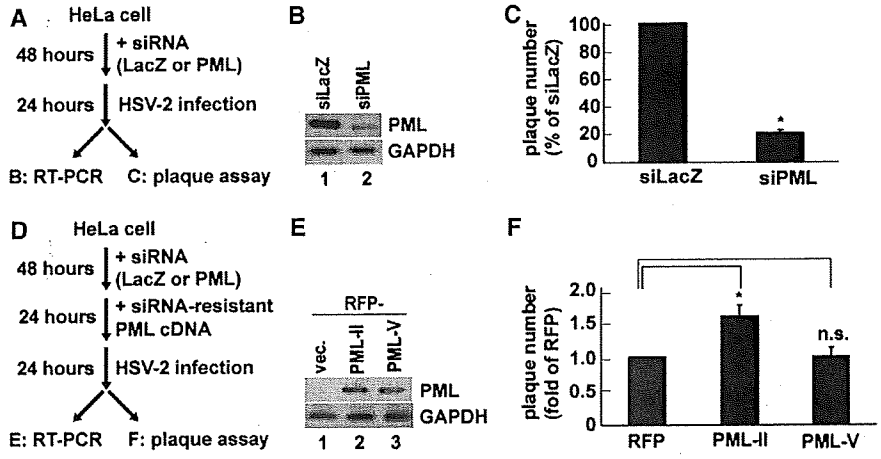

Figure 8. Differential function of PML isoforms in relation to HSV-2 infection. (A) Experimental procedure for examining the role of PML in HSV-2 viral production. Knockdown of all endogenous PML splicing variants in HeLa cells was performed using siRNA against PML (siPML4). After 48 h of incubation, HeLa cells were infected with HSV-2 at MOI 0.01 for 24 h. RT–PCR analysis (B) and plaque assay (C) were performed to determine knockdown efficiency and viral titer, respectively. (B) RT–PCR analysis, using PML ex3-ex4 primers, of siLacZ- or siPML4-treated HeLa cells. (C) Production of infectious HSV-2 in either siLacZ- or siPML4-treated HeLa cells as assessed by plaque assay ($n = 4$). (D) Experimental procedure for the rescue assay of PML splicing variants. After 48 h of siRNA treatment, the expression plasmids of either RFP or siRNA-resistant PML II or PML-V were transfected for 24 h. Following 24 h of infection with HSV-2 at MOI 0.01, RT–PCR analysis (E) and plaque assay (F) were performed. (E) RT–PCR analysis of siPML4-treated HeLa cells transfected with the RFP vector, RFP-PML-II siRNA resistant (siR), or RFP-PML-V siR expression plasmids. Details are described in 'Materials and Methods' section. (F) Production of infectious HSV-2 in HeLa cells siPML4-treated and then transfected with each PML plasmid as assessed by plaque assay ($n = 4$). $^*P < 0.001$; n.s., not significant.

pre-mRNA splicing. Interestingly, we observed that ICP27 specifically bound to PML pre-mRNA (Figure 5B, lane 5) and selectively switched the isoform from PML-II to PML-V by promoting the retention of PML intron 7a (Figure 3E). Our results indicate that ICP27 is an alternative splicing factor, although it does not inhibit all constitutive splicing. Moreover, the observed *in vitro* splicing suggested that ICP27 directly suppressed the early stage of spliceosome assembly on PML intron 7a, because splicing intermediates (5′ exon and lariat-3′ exon) were reduced by ICP27 addition (Figure 6F).

The selectivity of ICP27-dependent regulation may be related to the relative weakness of the 3′ ss of PML intron 7a. PML intron 7a was not retained even in the presence of ICP27 when we mutated the 3′ ss to the consensus sequence for U2AF65/35 (Figure 7B). Therefore, it is also relevant to examine whether ICP27 selectively binds to the 3′ ss of PML intron 7a by competing with U2AF65/35. Sokolowski *et al.* (52) showed that ICP27 binds to many different viral sequences by yeast three-hybrid screening of an HSV-1 genomic library; however, the target RNA sequence of ICP27 remains to be elucidated. Since the ICP27 homolog contains more cellular targets than PML pre-mRNA (53), *in vitro* systematic evolution of ligands by exponential enrichment (SELEX) and *in vivo* UV cross-linking immunoprecipitation (CLIP) are currently under way in our laboratory to determine the consensus target sequence of ICP27.

A possible role of ICP27-mediated mRNA export on alternative splicing

Transfection experiments revealed that ICP27 promoted the intron 7a retention (Figure 3B, lane 3). Although our results showed that ICP27 directly inhibited the splicing of PML intron 7a *in vitro* (Figure 6F), ICP27-mediated alternative splicing modulation is still possible to be explained by another mechanism, a promotion of pre-mRNA export by ICP27. It has been shown that ICP27 shuttles between the nucleus and the cytoplasm in host cells (54,55), and that ICP27 homologues stimulate the export of viral mRNAs by interacting with the mRNA export adaptor REF (56–61). The splicing reaction at the weak ss of PML intron 7a may take longer time than that at the consensus ss, and the accelerated mRNA export induced by ICP27 does not provide sufficient time for PML pre-mRNA to be spliced in the nucleus. These two possibilities are not mutually exclusive. It will be of interest to investigate if ICP27 promotes export of pre-mRNAs that harbor introns with weak 3′ ss, such as PML.

The role of ICP27 KH domain on PML alternative splicing

ICP27 M15 mutant failed to alter the expression of PML splicing isoform (Figure 4B, lane 7), suggesting that the KH3 domain is critical for the regulation of splicing. Therefore, we checked whether other KH domains are also essential for splicing regulation or not. RT–PCR analyses indicate that the mutants lacking either the KH2 domain or the KH3 domain were not able to completely switch PML splicing isoforms (data not shown). These results suggest that both the KH2 and the KH3 domains are required for altering the splicing. Unfortunately, the mutant lacking the KH1 domain was not expressed enough for the splicing experiment. It is highly likely that all of three KH domains are required for the regulation of the splicing.

Differential roles of PML isoform

PML isoforms have differential localizations and functions (32–34). For example, p53 interacts with PML-IV, but not with PML-III, and thus it was speculated that p53-PML-IV interaction was required for p53 recruitment into PML-NBs to modulate cell survival (62). Moreover, retinoblastoma protein (pRB) interacts more efficiently with PML-IV than with PML-II, suggesting that pRB–PML-IV interaction plays an important role in the regulation of cell differentiation and proliferation (63). In the present study, we showed that PML-II can enhance HSV-2 proliferation in HeLa cells (Figure 8F). In addition to HSV-2, adenovirus type 5 E4-ORF3 protein reportedly rearranges PML-NBs to a track-like structure by specifically interacting with PML-II (64,65), suggesting that PML-II may function as a modulator of the viral environment. However, as shown in the present study, HSV-2 infection switches the PML isoform from PML-II to PML-V. Apparently, this switching reduces the efficiency of viral replication (Figure 8F) and is thus not favorable to the virus, although it may also contribute to persistent viral infection by controlling viral replication rate through a negative feedback mechanism. Another possibility is that this switching is relevant to host defense to virus production. Because ICP27 is expressed at early stage of virus infection, the infected cell may utilize ICP27 as virus antigen to monitor virus infection and then the cells may try to reduce virus replication rate by producing PML-V, which results in delay of the expansion of virus infection to surrounding cells.

The expression of PML isoforms differs in various cell lines or tissues. For example, PML-I is the dominant form expressed in the brain but not in the liver (18). However, the regulation mechanisms of the cell type- or tissue-specific alternative splicing of PML pre-mRNA have not been clarified to date. In this study, using our original splicing reporter with RFP, we demonstrated that the viral protein ICP27 regulates the switching of the PML isoform from PML-II to PML-V by promoting the retention of PML intron 7a; PML-I, however, was not affected by ICP27 (Supplementary Figure S1A). The mechanism underlying the HSV-induced decrease in PML-I remains to be elucidated. The splicing reporter system used in the present study may pave the way for identifying the cellular regulators of PML alternative splicing, along with viral regulatory proteins.

SUPPLEMENTARY DATA

Supplementary Data are available at NAR Online.

ACKNOWLEDGEMENTS

We are grateful to H. de Thé for providing the anti-PML-II and PML-V specific sera. We thank A. Hiraishi and C. Parlayan for critically reading the article; and members of M.H.'s Laboratory for helpful comments.

FUNDING

Grants-in-Aid (to M.H.) from the Ministry of Education, Culture, Sports, Science, and Technology (MEXT) of Japan; the National Institute of Biomedical Innovation (NIBI); Japanese Ministry of Education, Global Center of Excellence (GCOE) Program; International Research Center for Molecular Science in Tooth and Bone Diseases; Program for Improvement of Research Environment for Young Researchers from Special Coordination Funds for Promoting Science and Technology (SCF) commissioned by MEXT of Japan (to N.K.). Funding for open access charge: [Ministry of Education, Culture, Sports, Science, and Technology of Japan (to T.N.)].

Conflict of interest statement. None declared.

REFERENCES

1. Johnson,J.M., Castle,J., Garrett-Engele,P., Kan,Z., Loerch,P.M., Armour,C.D., Santos,R., Schadt,E.E., Stoughton,R. and Shoemaker,D.D. (2003) Genome-wide survey of human alternative pre-mRNA splicing with exon junction microarrays. *Science*, **302**, 2141–2144.
2. Blencowe,B.J. (2006) Alternative splicing: new insights from global analyses. *Cell*, **126**, 37–47.
3. Black,D.L. (2003) Mechanisms of alternative pre-messenger RNA splicing. *Annu. Rev. Biochem.*, **72**, 291–336.
4. Matlin,A.J., Clark,F. and Smith,C.W. (2005) Understanding alternative splicing: towards a cellular code. *Nat. Rev. Mol. Cell Biol.*, **6**, 386–398.
5. Schwartz,S., Felber,B.K., Fenyo,E.M. and Pavlakis,G.N. (1990) Env and Vpu proteins of human immunodeficiency virus type 1 are produced from multiple bicistronic mRNAs. *J. Virol.*, **64**, 5448–5456.
6. Stoltzfus,C.M. and Madsen,J.M. (2006) Role of viral splicing elements and cellular RNA binding proteins in regulation of HIV-1 alternative RNA splicing. *Curr. HIV Res.*, **4**, 43–55.
7. Long,J.C. and Caceres,J.F. (2009) The SR protein family of splicing factors: master regulators of gene expression. *Biochem. J.*, **417**, 15–27.
8. Lin,S. and Fu,X.D. (2007) SR proteins and related factors in alternative splicing. *Adv. Exp. Med. Biol.*, **623**, 107–122.
9. Kanopka,A., Muhlemann,O., Petersen-Mahrt,S., Estmer,C., Ohrmalm,C. and Akusjarvi,G. (1998) Regulation of adenovirus alternative RNA splicing by dephosphorylation of SR proteins. *Nature*, **393**, 185–187.
10. Fukuhara,T., Hosoya,T., Shimizu,S., Sumi,K., Oshiro,T., Yoshinaka,Y., Suzuki,M., Yamamoto,N., Herzenberg,L.A., Herzenberg,L.A. *et al.* (2006) Utilization of host SR protein kinases and RNA-splicing machinery during viral replication. *Proc. Natl Acad. Sci. USA*, **103**, 11329–11333.
11. Ishov,A.M. and Maul,G.G. (1996) The periphery of nuclear domain 10 (ND10) as site of DNA virus deposition. *J. Cell Biol.*, **134**, 815–826.
12. de The,H., Lavau,C., Marchio,A., Chomienne,C., Degos,L. and Dejean,A. (1991) The PML-RAR alpha fusion mRNA generated by the t(15;17) translocation in acute promyelocytic leukemia encodes a functionally altered RAR. *Cell*, **66**, 675–684.
13. Kakizuka,A., Miller,W.H. Jr., Umesono,K., Warrell,R.P. Jr., Frankel,S.R., Murty,V.V., Dmitrovsky,E. and Evans,R.M. (1991) Chromosomal translocation t(15;17) in human acute promyelocytic leukemia fuses RAR alpha with a novel putative transcription factor, PML. *Cell*, **66**, 663–674.
14. Goddard,A.D., Borrow,J., Freemont,P.S. and Solomon,E. (1991) Characterization of a zinc finger gene disrupted by the t(15;17) in acute promyelocytic leukemia. *Science*, **254**, 1371–1374.
15. Gurrieri,C., Capodieci,P., Bernardi,R., Scaglioni,P.P., Nafa,K., Rush,L.J., Verbel,D.A., Cordon-Cardo,C. and Pandolfi,P.P. (2004)

Loss of the tumor suppressor PML in human cancers of multiple histologic origins. *J. Natl Cancer Inst.*, **96**, 269–279.
16. Terris,B., Baldin,V., Dubois,S., Degott,C., Flejou,J.F., Henin,D. and Dejean,A. (1995) PML nuclear bodies are general targets for inflammation and cell proliferation. *Cancer Res.*, **55**, 1590–1597.
17. Koken,M.H., Linares-Cruz,G., Quignon,F., Viron,A., Chelbi-Alix,M.K., Sobczak-Thepot,J., Juhlin,L., Degos,L., Calvo,F. and de The,H. (1995) The PML growth-suppressor has an altered expression in human oncogenesis. *Oncogene*, **10**, 1315–1324.
18. Condemine,W., Takahashi,Y., Zhu,J., Puvion-Dutilleul,F., Guegan,S., Janin,A. and de The,H. (2006) Characterization of endogenous human promyelocytic leukemia isoforms. *Cancer Res.*, **66**, 6192–6198.
19. Salomoni,P. and Pandolfi,P.P. (2002) The role of PML in tumor suppression. *Cell*, **108**, 165–170.
20. Zhong,S., Salomoni,P. and Pandolfi,P.P. (2000) The transcriptional role of PML and the nuclear body. *Nat. Cell Biol*, **2**, E85–E90.
21. Hofmann,T.G. and Will,H. (2003) Body language: the function of PML nuclear bodies in apoptosis regulation. *Cell Death Differ.*, **10**, 1290–1299.
22. Guo,A., Salomoni,P., Luo,J., Shih,A., Zhong,S., Gu,W. and Pandolfi,P.P. (2000) The function of PML in p53-dependent apoptosis. *Nat. Cell Biol.*, **2**, 730–736.
23. Dellaire,G. and Bazett-Jones,D.P. (2004) PML nuclear bodies: dynamic sensors of DNA damage and cellular stress. *Bioessays*, **26**, 963–977.
24. Ching,R.W., Dellaire,G., Eskiw,C.H. and Bazett-Jones,D.P. (2005) PML bodies: a meeting place for genomic loci? *J. Cell Sci.*, **118**, 847–854.
25. Pearson,M., Carbone,R., Sebastiani,C., Cioce,M., Fagioli,M., Saito,S., Higashimoto,Y., Appella,E., Minucci,S., Pandolfi,P.P. *et al.* (2000) PML regulates p53 acetylation and premature senescence induced by oncogenic Ras. *Nature*, **406**, 207–210.
26. Wang,Z.G., Delva,L., Gaboli,M., Rivi,R., Giorgio,M., Cordon-Cardo,C., Grosveld,F. and Pandolfi,P.P. (1998) Role of PML in cell growth and the retinoic acid pathway. *Science*, **279**, 1547–1551.
27. Lin,H.K., Bergmann,S. and Pandolfi,P.P. (2004) Cytoplasmic PML function in TGF-beta signalling. *Nature*, **431**, 205–211.
28. Everett,R.D. (2001) DNA viruses and viral proteins that interact with PML nuclear bodies. *Oncogene*, **20**, 7266–7273.
29. Regad,T. and Chelbi-Alix,M.K. (2001) Role and fate of PML nuclear bodies in response to interferon and viral infections. *Oncogene*, **20**, 7274–7286.
30. Chee,A.V., Lopez,P., Pandolfi,P.P. and Roizman,B. (2003) Promyelocytic leukemia protein mediates interferon-based anti-herpes simplex virus 1 effects. *J. Virol.*, **77**, 7101–7105.
31. Maul,G.G., Ishov,A.M. and Everett,R.D. (1996) Nuclear domain 10 as preexisting potential replication start sites of herpes simplex virus type-1. *Virology*, **217**, 67–75.
32. Jensen,K., Shiels,C. and Freemont,P.S. (2001) PML protein isoforms and the RBCC/TRIM motif. *Oncogene*, **20**, 7223–7233.
33. Nisole,S., Stoye,J.P. and Saib,A. (2005) TRIM family proteins: retroviral restriction and antiviral defence. *Nat. Rev.*, **3**, 799–808.
34. Condemine,W., Takahashi,Y., Le Bras,M. and de The,H. (2007) A nucleolar targeting signal in PML-I addresses PML to nucleolar caps in stressed or senescent cells. *J. Cell Sci.*, **120**, 3219–3227.
35. Kuroyanagi,H., Kobayashi,T., Mitani,S. and Hagiwara,M. (2006) Transgenic alternative-splicing reporters reveal tissue-specific expression profiles and regulation mechanisms in vivo. *Nat. Methods*, **3**, 909–915.
36. Ohno,G., Hagiwara,M. and Kuroyanagi,H. (2008) STAR family RNA-binding protein ASD-2 regulates developmental switching of mutually exclusive alternative splicing in vivo. *Genes Dev.*, **22**, 360–374.
37. Tanaka,M., Kagawa,H., Yamanashi,Y., Sata,T. and Kawaguchi,Y. (2003) Construction of an excisable bacterial artificial chromosome containing a full-length infectious clone of herpes simplex virus type 1: viruses reconstituted from the clone exhibit wild-type properties in vitro and in vivo. *J. Virol.*, **77**, 1382–1391.
38. Sugimoto,K., Uema,M., Sagara,H., Tanaka,M., Sata,T., Hashimoto,Y. and Kawaguchi,Y. (2008) Simultaneous tracking of capsid, tegument, and envelope protein localization in living cells infected with triply fluorescent herpes simplex virus 1. *J. Virol.*, **82**, 5198–5211.
39. Tanaka,M., Kodaira,H., Nishiyama,Y., Sata,T. and Kawaguchi,Y. (2004) Construction of recombinant herpes simplex virus type I expressing green fluorescent protein without loss of any viral genes. *Microbes Infect./Institut Pasteur*, **6**, 485–493.
40. Krainer,A.R., Maniatis,T., Ruskin,B. and Green,M.R. (1984) Normal and mutant human beta-globin pre-mRNAs are faithfully and efficiently spliced in vitro. *Cell*, **36**, 993–1005.
41. Strom,T. and Frenkel,N. (1987) Effects of herpes simplex virus on mRNA stability. *J. Virol.*, **61**, 2198–2207.
42. Rice,S.A. and Lam,V. (1994) Amino acid substitution mutations in the herpes simplex virus ICP27 protein define an essential gene regulation function. *J. Virol.*, **68**, 823–833.
43. Soliman,T.M. and Silverstein,S.J. (2000) Herpesvirus mRNAs are sorted for export via Crm1-dependent and -independent pathways. *J. Virol.*, **74**, 2814–2825.
44. Sedlackova,L., Perkins,K.D., Lengyel,J., Strain,A.K., van Santen,V.L. and Rice,S.A. (2008) Herpes simplex virus type 1 ICP27 regulates expression of a variant, secreted form of glycoprotein C by an intron retention mechanism. *J. Virol.*, **82**, 7443–7455.
45. Majerciak,V., Yamanegi,K., Allemand,E., Kruhlak,M., Krainer,A.R. and Zheng,Z.M. (2008) Kaposi's sarcoma-associated herpesvirus ORF57 functions as a viral splicing factor and promotes expression of intron-containing viral lytic genes in spliceosome-mediated RNA splicing. *J. Virol.*, **82**, 2792–2801.
46. Wu,S., Romfo,C.M., Nilsen,T.W. and Green,M.R. (1999) Functional recognition of the 3' splice site AG by the splicing factor U2AF35. *Nature*, **402**, 832–835.
47. Sacks,W.R., Greene,C.C., Aschman,D.P. and Schaffer,P.A. (1985) Herpes simplex virus type 1 ICP27 is an essential regulatory protein. *J. Virol.*, **55**, 796–805.
48. Rice,S.A. and Knipe,D.M. (1988) Gene-specific transactivation by herpes simplex virus type 1 alpha protein ICP27. *J. Virol.*, **62**, 3814–3823.
49. Sandri-Goldin,R.M. and Hibbard,M.K. (1996) The herpes simplex virus type 1 regulatory protein ICP27 coimmunoprecipitates with anti-Sm antiserum, and the C terminus appears to be required for this interaction. *J. Virol.*, **70**, 108–118.
50. Sciabica,K.S., Dai,Q.J. and Sandri-Goldin,R.M. (2003) ICP27 interacts with SRPK1 to mediate HSV splicing inhibition by altering SR protein phosphorylation. *EMBO J.*, **22**, 1608–1619.
51. Bryant,H.E., Wadd,S.E., Lamond,A.I., Silverstein,S.J. and Clements,J.B. (2001) Herpes simplex virus IE63 (ICP27) protein interacts with spliceosome-associated protein 145 and inhibits splicing prior to the first catalytic step. *J. Virol.*, **75**, 4376–4385.
52. Sokolowski,M., Scott,J.E., Heaney,R.P., Patel,A.H. and Clements,J.B. (2003) Identification of herpes simplex virus RNAs that interact specifically with regulatory protein ICP27 in vivo. *J. Biol. Chem.*, **278**, 33540–33549.
53. Verma,D. and Swaminathan,S. (2008) Epstein-Barr virus SM protein functions as an alternative splicing factor. *J. Virol.*, **82**, 7180–7188.
54. Phelan,A. and Clements,J.B. (1997) Herpes simplex virus type 1 immediate early protein IE63 shuttles between nuclear compartments and the cytoplasm. *J. Gen. Virol.*, **78(Pt 12)**, 3327–3331.
55. Mears,W.E. and Rice,S.A. (1998) The herpes simplex virus immediate-early protein ICP27 shuttles between nucleus and cytoplasm. *Virology*, **242**, 128–137.
56. Hiriart,E., Farjot,G., Gruffat,H., Nguyen,M.V., Sergeant,A. and Manet,E. (2003) A novel nuclear export signal and a REF interaction domain both promote mRNA export by the Epstein-Barr virus EB2 protein. *J. Biol. Chem.*, **278**, 335–342.
57. Malik,P., Blackbourn,D.J. and Clements,J.B. (2004) The evolutionarily conserved Kaposi's sarcoma-associated herpesvirus ORF57 protein interacts with REF protein and acts as an RNA export factor. *J. Biol. Chem.*, **279**, 33001–33011.
58. Williams,B.J., Boyne,J.R., Goodwin,D.J., Roaden,L., Hautbergue,G.M., Wilson,S.A. and Whitehouse,A. (2005) The prototype gamma-2 herpesvirus nucleocytoplasmic shuttling protein, ORF 57, transports viral RNA through the cellular mRNA export pathway. *Biochem. J.*, **387**, 295–308.

59. Lischka,P., Toth,Z., Thomas,M., Mueller,R. and Stamminger,T. (2006) The UL69 transactivator protein of human cytomegalovirus interacts with DEXD/H-Box RNA helicase UAP56 to promote cytoplasmic accumulation of unspliced RNA. *Mol. Cell Biol.*, **26**, 1631–1643.
60. Soliman,T.M., Sandri-Goldin,R.M. and Silverstein,S.J. (1997) Shuttling of the herpes simplex virus type 1 regulatory protein ICP27 between the nucleus and cytoplasm mediates the expression of late proteins. *J. Virol.*, **71**, 9188–9197.
61. Koffa,M.D., Clements,J.B., Izaurralde,E., Wadd,S., Wilson,S.A., Mattaj,I.W. and Kuersten,S. (2001) Herpes simplex virus ICP27 protein provides viral mRNAs with access to the cellular mRNA export pathway. *EMBO J.*, **20**, 5769–5778.
62. Fogal,V., Gostissa,M., Sandy,P., Zacchi,P., Sternsdorf,T., Jensen,K., Pandolfi,P.P., Will,H., Schneider,C. and Del Sal,G. (2000) Regulation of p53 activity in nuclear bodies by a specific PML isoform. *EMBO J.*, **19**, 6185–6195.
63. Alcalay,M., Tomassoni,L., Colombo,E., Stoldt,S., Grignani,F., Fagioli,M., Szekely,L., Helin,K. and Pelicci,P.G. (1998) The promyelocytic leukemia gene product (PML) forms stable complexes with the retinoblastoma protein. *Mol. Cell Biol.*, **18**, 1084–1093.
64. Doucas,V., Ishov,A.M., Romo,A., Juguilon,H., Weitzman,M.D., Evans,R.M. and Maul,G.G. (1996) Adenovirus replication is coupled with the dynamic properties of the PML nuclear structure. *Genes Dev.*, **10**, 196–207.
65. Hoppe,A., Beech,S.J., Dimmock,J. and Leppard,K.N. (2006) Interaction of the adenovirus type 5 E4 Orf3 protein with promyelocytic leukemia protein isoform II is required for ND10 disruption. *J. Virol.*, **80**, 3042–3049.

Akt2 Regulation of Cdc2-Like Kinases (Clk/Sty), Serine/Arginine-Rich (SR) Protein Phosphorylation, and Insulin-Induced Alternative Splicing of PKCβII Messenger Ribonucleic Acid

Kun Jiang, Niketa A. Patel, James E. Watson, Hercules Apostolatos, Eden Kleiman, Olivia Hanson, Masatoshi Hagiwara, and Denise R. Cooper

Department of Molecular Medicine (K.J., N.A.P., H.A., E.K., D.R.C.), University of South Florida College of Medicine, and Research Service (N.A.P., J.E.W., D.R.C.), J. A. Haley Veterans Hospital, Tampa, Florida 33612; Department of Chemistry (O.H.), University of Central Oklahoma, Edmond, Oklahoma 73034; and Laboratory of Gene Expression (M.H.), School of Biomedical Science, Department of Functional Genomics, Medical Research Institute, Tokyo Medical and Dental University, Bunkyo-Ku Tokyo 113-8510, Japan

Serine/arginine-rich (SR) proteins play essential roles in the constitutive and regulated splicing of precursor mRNAs. Phosphorylation of the arginine/serine dipeptide-rich (RS) domain by SR protein kinases such as Cdc2-like kinases (Clk/Sty) modulates their subcellular localization and activation. However, it remains unclear how these kinases and their target SR proteins are regulated by extracellular signals. Regulation of protein kinase C βII (PKCβII) pre-mRNA alternative splicing via exon inclusion by Akt2, a central kinase in insulin action, involves phosphorylation of SR proteins. Here we showed that Akt2, in response to insulin, resulted in phosphorylation of Clk/Sty, which then altered SR protein phosphorylation in concert with Akt2. Insulin-stimulated PKCβII pre-mRNA splicing was blocked by Clk/Sty and phosphatidylinositol-3-kinase inhibitors, and diabetic Akt2-null mouse tissues had impaired phospho-Clk/Sty, SR protein phosphorylation, and PKCβII expression. Furthermore, we observed that Akt2 phosphorylated several SR proteins distinct from Clk/Sty in response to insulin. Akt2-catalyzed phosphorylation of Clk/Sty and SR proteins revealed a role for both kinases in splicing regulation indicating dual functions for Akt2 in response to insulin in this pathway. (***Endocrinology*** **150: 2087–2097, 2009)**

Alternative pre-mRNA splicing provides a versatile mechanism in gene expression and proteome diversity. It is also a means of diversifying signaling pathways when kinases, such as protein kinase C (PKC) β, are the target genes. Phosphorylated serine/arginine-rich (SR) proteins function as exon splicing enhancers and repressors within the spliceosomal complex. This family of proteins plays pivotal roles in constitutive and regulated splicing (1), because they are located at the center of the regulatory pathways that lead to the selection of alternative splice sites. The various kinases that regulate the phosphorylation, intranuclear distribution, and protein-protein interactions of SR proteins play key roles in selection of alternative splice sites (1–3). Recently, Akt2 or PKB, an oncogene originally isolated from retrovirus AKT8-induced mouse thymic lymphoma, was shown to regulate alternative splicing (4, 5). Additionally, SR protein-specific kinases (SRPK), CDC2-like kinases (Clk), cAMP-dependent protein kinase (PKA), and PKC all phosphorylate splicing factors containing Arg/Ser repeat motifs and have the potential to regulate splicing (6–8). The Clk kinases participate in a network of regulatory mechanisms that enable SR proteins to control RNA splicing in response to phosphorylation (7–10).

Clk/Sty kinase controls splicing during cellular proliferation and differentiation (11–13). Clk/Sty (Clk1) and Clk2, Clk3, and Clk4 are phosphorylated on serine/threonine and tyrosine residues (7), and they contain Akt-substrate motifs, implying that Clk could be regulated by the phosphatidylinositol 3-kinase (PI3K)/Akt pathway and that this alters their substrate specific-

ISSN Print 0013-7227 ISSN Online 1945-7170
Printed in U.S.A.

doi: 10.1210/en.2008-0818 Received June 2, 2008. Accepted December 23, 2008.
First Published Online December 30, 2008

Abbreviations: Clk, CDC2-like kinase; DMSO, dimethylsulfoxide; FBS, fetal bovine serum; HA, hemagglutinin; PI3K, phosphatidylinositol 3-kinase; PKC, protein kinase C; siRNA, small interfering RNA; SR, serine/arginine-rich; SRPK, SR protein-specific kinase.

ity. However, no upstream kinase has been shown to regulate Clk/Sty function, thus limiting our understanding of its regulatory roles.

The unique mechanism that underlies alternative splicing of PKCβ pre-mRNA has been well documented in mammalian cells and animal models (14–17); these studies implicated Clk/Sty in splicing of PKCβII mRNA, a step necessary for insulin action (18–20). Insulin stimulates the inclusion of an exon encoding the C-terminal domain of PKCβII; PKCβI is the other splice variant. The pathway involves PI3K/Akt2-mediated phosphorylation of multiple SR proteins, including SRp40 (5). SR proteins, within their Arg/Ser domains, contain the highest number of Akt consensus motifs found in proteins (21). Regulation of alternative splicing and gene expression by PDK/Akt provides a unique modulation of growth factor action at the level of extracellular signaling (22–24). Because Clk/Sty contains two Akt consensus motifs, Arg-Xaa-Arg-Xaa-Xaa-(Ser/Thr), we hypothesized that its activity might be regulated by insulin and, furthermore, that Akt phosphorylation of Clk/Sty was necessary for the regulation of PKCβII exon inclusion.

Materials and Methods

Materials

Tissue culture medium was purchased from Invitrogen (Carlsbad, CA). Fetal bovine serum (FBS) was purchased from Atlanta Biologicals (Norcross, GA). Porcine insulin was from Sigma Chemical Co. (St. Louis, MO). Reagents for polyacrylamide gel electrophoresis were from Bio-Rad (Hercules, CA). SRp75 polyclonal antibody was raised in rabbits to the synthetic peptide NH_2-(GC)KDHAEDKLQNNDSAGKAK-COOH (residues 119–136), SRp30b/SC35 antibody to the synthetic peptide NH_2-CRRVGDVYIPRDRYTKE-COOH (residues 38–53), and SRp55 antibody to the synthetic peptide NH_2-CGERVIVEHARGPRRDRD-COOH (residues 61–78) by Bio-Synthesis, Inc. (Louisville, TX). Antibodies were characterized alongside unreactive preimmune antisera and were shown to recognize rat, mouse, and human cell line proteins. Antibody to a phospho-epitope in all SR proteins (mAb104) was obtained from hybridoma cells (CRL 2067; American Type Culture Collection, Manassas, VA). Anti-phospho-Akt (Ser473 and Akt antibody) and anti-Akt substrate (RXRXXS/T) antibody were from Cell Signaling (Beverly, MA). Anti-Clk/Sty antibody was kindly provided by Dr. James Manley (Columbia University, New York, NY). Enhanced chemiluminescence reagents were from Pierce (Rockford, IL). *Taq* Platinum polymerase was from PerkinElmer Life Sciences (Norwalk, CT). Lipofectin was from Invitrogen. PI3K inhibitor LY294002 and Src kinase inhibitor PP1 were purchased from Calbiochem (La Jolla, CA). All other chemicals and reagents were purchased from the usual vendors. PP1 is preincubated with cells for 30 min before addition of insulin. LY294002 and PP1 were preincubated with cells for 30 min before addition of insulin.

Cell lines and Akt2-null tissues

L6 rat skeletal myoblasts were obtained from Dr. Amira Klip (The Hospital for Sick Children, Toronto, Canada) and were grown in α-MEM containing 10% FBS at 37 C in a humidified 5% CO_2, 95% air atmosphere in either six-well or 100-mm plates. Cells were grown to 80% confluency and induced to differentiate into multinucleated myotubes by reducing the FBS to 2% for 6 d before the experiment. Cells were then washed with PBS and incubated in serum-free α-MEM for 6 h before each experiment. Porcine insulin (Sigma) was used at a final concentration of 10 nM and, unless otherwise stated, was added to the cells 30 min before cell lysis. COS7 cells were grown in DMEM containing 10% FBS as stated above.

Akt2-null mouse tissues were provided by Dr. Morris J. Birnbaum (Howard Hughes Medical Institute, Department of Medicine, University of Pennsylvania School of Medicine, Philadelphia, PA). Akt2-null and wild-type tissues were obtained from fasted 24 week old male animals raised at the Chemerie Mouse Facility at University of Pennsylvania, an AALAC accredited facility. Akt2-null mice were impaired in the ability of insulin to lower blood glucose because of defects in the action of the hormone on liver and skeletal muscle (25).

Transient transfection of plasmid DNA or small interfering RNA (siRNA)

Hemagglutinin (HA)-Clk/Sty-expressing cDNA plasmid was obtained from Dr. James Manley (Department of Biology, Columbia University, New York, NY) (13). HA-Akt2 has been described previously (5, 26). Plasmid DNA or siRNA (Ambion, Austin, TX; series 1: Clk1 ID#161218, Akt2 ID#200808; series 2: Alk1 ID#16704 and Akt2 ID#200807) was transfected into cells at 60–80% confluency using Lipofectin (Invitrogen) or siPORT Amine (Ambion) for 5 h as per manufacturer's instructions. Cells were then maintained in α-MEM with 2% FBS for 30 h and serum starved 6 h before insulin addition. Expression of exogenous genes was demonstrated by Western blot analysis using the appropriate antibody. The transfection efficiency of L6 myotubes was routinely shown to be above 60% (19).

Immunoprecipitation

L6 myotubes, COS7 cell pellets, or mouse tissue samples were lysed in 20 vol 150 mM NaCl, 1% Triton X-100, 0.5% sodium deoxycholate, 0.1% sodium dodecyl sulfate, and 50 mM Tris (pH 8.0) with the following protease inhibitors: benzamidine HCl, 16 μg/ml; aprotinin, 10 μg/ml; leupeptin; 10 μg/ml; and phenylmethylsulfonyl fluoride, 1 mM. The mixtures were placed on ice for 30 min, and insoluble material was pelleted at 12,000 × *g* for 10 min at 4 C. An aliquot (500 μg) of lysate was incubated at a final concentration of 1 μg/μl with anti-Clk/Sty polyclonal antibody followed by agitation at 4 C for 2 h. A 40-μl aliquot of protein A-Sepharose beads in a 1:1 suspension with the lysis buffer was added and incubated again for 1 h. After centrifugation at 10,000 × *g*, beads were washed four times with 1 ml lysis buffer containing 0.5 M NaCl, followed by a wash in lysis buffer with no NaCl. After adding 50 μl SDS-PAGE sample buffer, the precipitate was boiled for 5 min and centrifuged at 1000 rpm for 5 min before loading on the gel followed by Western blot analysis.

Western blot

Cell or tissue lysates (40 μg) or immunoprecipitates obtained from 500 μg lysates were separated on 10% SDS-PAGE. Proteins were electrophoretically transferred to nitrocellulose membranes, blocked with Tris-buffered saline-0.1% Tween 20 containing 5% nonfat dried milk, washed, and incubated with a polyclonal antibody against SRp75, SRp55, SRp30b, or mAb104, a monoclonal antibody against the phospho-epitope (RS domain) of SR proteins (27), Akt, anti-phospho-Akt, anti-phospho-ERK1/2 (Cell Signaling), anti-HA (Roche, Indianapolis, IN), or anti-Clk/Sty (Dr. James Manley, Columbia University, New York, NY). Anti-phosphotyrosine antibody 4G10 was purchased from Upstate (Lake Placid, NY). After incubation with secondary antirabbit or antimouse IgG-horseradish peroxidase, detection was performed using enhanced chemiluminescence (Pierce). In all cases, Western blot results were verified in two to four separate experiments.

RT-PCR analysis for PKCβII

Splice products were detected as reported earlier (5). Briefly, total RNA (1 μg) was used to synthesize first-strand cDNA using an oligo(dT) primer and Omniscript II reverse transcriptase (QIAGEN, Valencia, CA). Inclusion of the PKCβII-specific exon was detected using a sense primer corresponding to the V3 domain 5′-ATGAAACTGACCGATTT-TAACTT-3′ and antisense primer (βII specific) for V5 domain (5′-CG-GAGGTCTACAGATCTACTTAGCTCT-3′). After 35 cycles of the

PCR amplification program (95 C for 30 sec, 54 C for 30 sec, and 72 C for 45 sec) using *Taq* Platinum DNA polymerase (PerkinElmer), 5% of the PCR was resolved by electrophoresis on 6% polyacrylamide gels, and fragments were detected by silver staining. The resulting product was 1044 bp. The reaction was optimized for linear range amplification. The Kodak (Rochester, NY) Digital Analysis System 120 was used to visualize PCR products. The results were verified in two separate experiments. PCR fragments were quantified using UnScan software (Silk Scientific, Orem, UT).

Measurement of insulin-stimulated glucose transport by 2-deoxyglucose uptake

L6 myoblasts were grown and differentiated as described above in 24-well plates. Cells were then washed with PBS and incubated in serum-free α-MEM for 4 h before each experiment. The inhibitor was added 2 h before each experiment. Cells were then washed and incubated in PBS with 1% BSA at 37 C with inhibitors and/or 50 nM insulin (Sigma) 30 min before the addition of 10 nmol [^{3}H]2-deoxyglucose (50–150 μCi/μmol) and incubation for 6 min at 37 C. Cells were then washed three times with ice-cold PBS and lysed in 1% sodium dodecyl sulfate. Radioactivity was determined by liquid scintillation counting.

Results

A role for Clk/Sty in splicing of PKCβ mRNA

PKCβI and PKCβII are the products of alternative splicing of PKCβ pre-mRNA. The last common exon of the C4 domain (exon 16) splices to the βIV5 exon (exon 18) to produce PKCβI mRNA, which is constitutively expressed. Insulin regulates the inclusion of PKCβII exon (exon 17) between the C4 and βIV5 domains, thereby producing mature PKCβII mRNA. The βI exon then becomes 3′-untranslated region on PKCβII mRNA due to a stop codon within the βII exon. Insulin exerts some of its effects on alternative splicing via Akt2 phosphorylation of SRp40, a nuclear splicing factor (5). The notion that Clk/Sty might also be involved in the insulin response was suggested from the observation that the splicing of PKCβII pre-mRNA is accompanied by phosphorylation of multiple SR proteins (14), and Clk/Sty influences the activity of SR proteins (11–13). Our previous studies using a heterologous PKCβII splicing minigene demonstrated that βII exon inclusion is regulated by insulin and minigene exon inclusion is mimicked by Clk/Sty overexpression (14–17). Here, the selective Clk/Sty inhibitor TG003 was used to block its activity in L6 myotubes to demonstrate a role for the kinase in insulin action. TG003, a benzothiazole kinase inhibitor that targets Clk/Sty, is capable of suppressing dissociation of nuclear speckles, altering splicing patterns, and rescues embryonic defects induced by excessive Clk activity (28). Dimethylsulfoxide (DMSO), the solvent control, did not affect PKCβII splicing. TG009, the control compound (28), also did not affect splicing (data not shown). TG003 blocked insulin-stimulatory effects on βII exon inclusion (Fig. 1A). This suggested that Clk/Sty was involved in the splicing signal cascade.

Cells overexpressing Clk/Sty increased exon 17 (βII exon) inclusion (Fig. 1B). PKCβII protein expression (Western blot in Fig. 1B) was also elevated in a manner similar to that of insulin. When cells overexpressing Clk/Sty were treated with LY294002, an inhibitor known to block Akt2 activation and Akt2-mediated exon inclusion (11), βII exon inclusion was blocked (Fig. 1B),

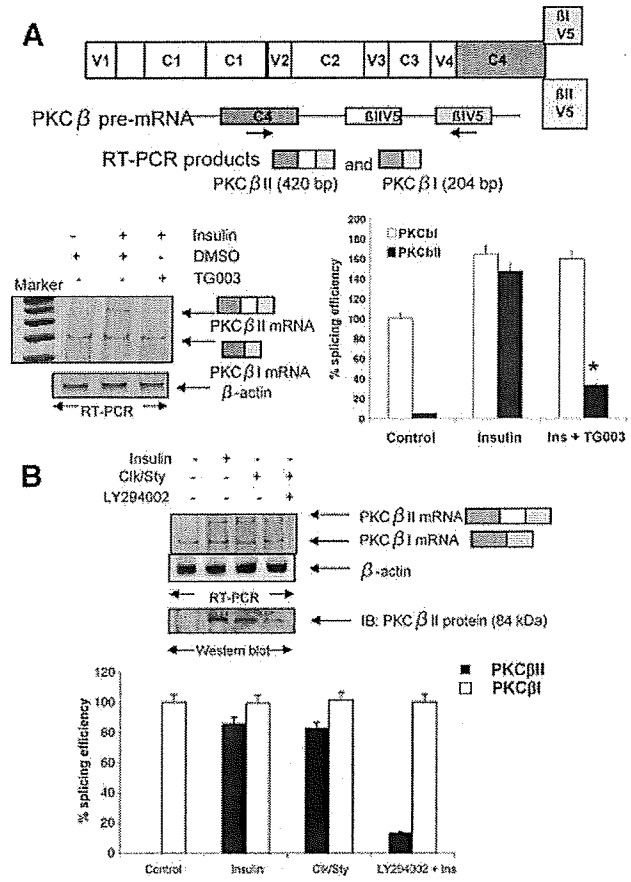

FIG. 1. Role of Clk/Sty and Akt2 in PKCβII exon inclusion. A, Schematic shows PKCβ domains and C-terminal alternative exons. *Arrow below* exons indicates the primer positions on PKCβ pre-mRNA. The primer set allowed for simultaneous detection of endogenous PKCβI mRNA and βII mRNA (in which βII exon is included between C4 and βI exon). After serum starvation for 6 h, differentiated L6 myotubes were treated with TG003 (10 μM) for 60 min before insulin addition (10 nM, 30 min). DMSO served as the solvent control. Total RNA was extracted and 2 μg analyzed for PKCβI and PKCβII by RT-PCR using primers corresponding to the C4 and βI/V5 exon as shown on the diagram. β-Actin was amplified as an internal control. Clk/Sty inhibitor blocked insulin-stimulated PKCβII exon inclusion. The graph represents three separate experiments analyzed by RT-PCR. *, $P < 0.05$ by Student's t test. B, Clk/Sty-induced PKCβII exon inclusion was blocked by the PI3K inhibitor LY294002. L6 myotubes were transfected with Clk/Sty cDNA-expressing construct for 36 h and treated with insulin (Ins; 10 nM, 30 min) in the presence or absence of LY294002 (10 μM, 30 min). Endogenous PKCβI and PKCβII mRNA levels were amplified by RT-PCR as described in A. Cell lysates from duplicate plates were analyzed for protein levels of PKCβII by Western blot analysis after SDS-PAGE. The graph is representative of three RT-PCR analyses. Percent splicing efficiency is calculated as a ratio of PKCβII/βI mRNA with control PKCβI mRNA assigned a value of 100%.

suggesting that Akt2 was acting upstream of Clk/Sty. Densitometric scans of the PCR products indicated the block of exon inclusion by LY294002. PKCβI levels were not changed, as noted in earlier studies demonstrating the primary effect of insulin to be on exon inclusion rather than transcription (14).

Splicing was also assessed with a heterologous minigene containing the PKCβII exon and its flanking intronic sequences. To provide evidence that the Clk/Sty inhibitor effects may be explained by its inhibitory actions on Clk/Sty, Clk/Sty and Akt2 siRNA were used to lower intracellular kinase levels in combination and alone in the presence of insulin. Insulin-induced inclusion of the PKCβII exon in the heterologous minigene was

blocked more than 90% in the presence of both Clk/Sty and Akt2 siRNA and more than 75% in the presence of either kinase siRNA alone (Fig. 2A). Insulin also activates a second splice site, SSII, which is easier to detect with the minigene (17). The combined siRNA reduced levels of SSII product entirely. This suggested that there are differences in splice site regulation with regard to Akt2 and Clk/Sty. A second series of Clk/Sty and Akt2 siRNA confirmed the siRNA lowered the respective kinase levels, and the effects on splicing were not likely due to off-target knockdown by the complementary strand of DNA (Fig. 2B). The partial activation of an alternative 5′ splice site was still noted with Clk/Sty and Akt2 siRNA (series 2), suggesting roles for both kinases. Activation of both 5′ splice sites is also regulated by insulin (17), although only one protein is translated because there is a stop codon upstream of the first splice site. The longer mRNA is predicted to be more stable because it would not be subject to degradation (29). The inhibition of Clk/Sty and Akt2 blocked alternative exon inclusion and not merely splicing, because SD-SA splicing (vector splice sites) was not affected.

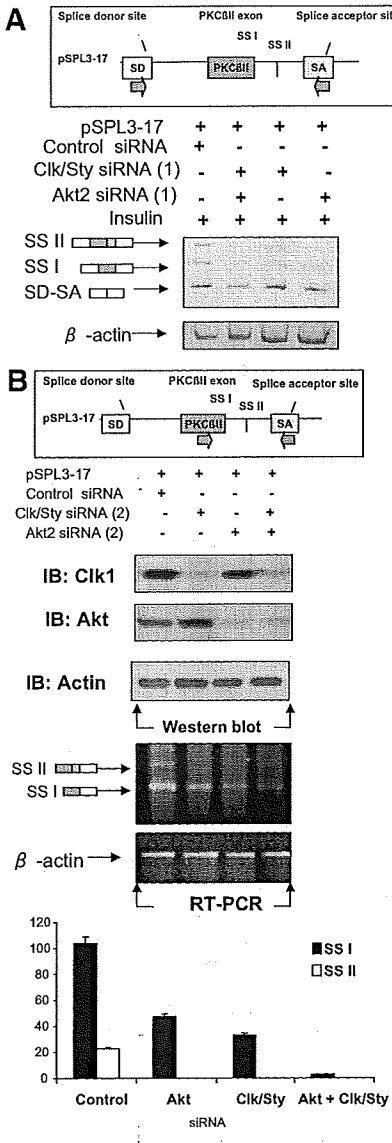

FIG. 2. Clk/Sty and Akt2 siRNA block splicing of heterologous minigene. A, Heterologous splicing vector and siRNA. L6 myotubes were cotransfected with pSPL3-17 splicing vector (18), Clk/Sty, and/or Akt2 siRNA (Silencer siRNA 161218 and 200808 or the control siRNA, 15 nM for 48 h) with Lipofectamine. After 6 h serum starvation, cells were treated with insulin (10 nM, 30 min). Total RNA was extracted, and PKCβII exon inclusion was analyzed using primers to the splice site donor and acceptor (18) as shown. SSI, Utilization of PKCβII exon 5′ splice site I; SSII, utilization of PKCβII exon 5′ splice site II; SD (splice donor)-SA (splice acceptor), constitutive splicing of pSPL3 splicing vector, which also serves as an internal control. The effectiveness of the siRNA (series 1) in lowering protein levels is shown in Fig. 4. The densitometric scan of the image indicates that the combined Clk/Sty and Akt2 siRNA were additive in blocking splice site 1. B, A second set of Clk/Sty siRNA and Akt2 siRNA also blocked splicing. L6 myotubes were cotransfected with pSPL3-17 splicing vector (18), Clk/Sty, and/or Akt2 siRNA (Silencer siRNA 161219 and 100807 or the control siRNA, 15 nM for 48 h) with Lipofectamine and treated as described above. The effectiveness of the siRNA in lowering protein levels is shown on the *top*, and the splicing of the minigene in the presence of both siRNA is shown on the *bottom*.

Phosphorylation of Clk/Sty by Akt

The possibility of Akt2 regulating Clk/Sty was examined because LY294002 blocked Clk-induced βII exon inclusion in Fig. 1B. Both serine and tyrosine phosphorylation of Clk/Sty are required for its full activation (11–13). However, the kinases regulating its activity have not been identified. The possible phosphorylation and activation of Clk/Sty by PI3K/Akt2 and Src tyrosine kinases was examined in COS7 cells. COS7 cells are easily transfected, and insulin signaling pathways have been demonstrated for them (30). COS7 cells were cotransfected with HA-tagged Akt2 and HA-tagged Clk/Sty before treatment with LY294002 or PP1 (an inhibitor of Src kinases), and then stimulated with insulin. Clk/Sty immunoprecipitates were analyzed by immunoblot using an antibody that specifically detects phosphorylation of serines in the Akt substrate motif and with another antibody that detects phosphorylated tyrosine residues. Insulin stimulated both Akt-motif serine and tyrosine phosphorylation of Clk/Sty (Fig. 3A, a and b), and the insulin-stimulated phosphorylation was suppressed by the PI3K inhibitor LY294002 and by the Src kinase inhibitor PP1 (lanes 4 and 5), respectively. Insulin was required to activate transfected Akt2 because in the absence of insulin, there was no phosphorylation of Clk (Fig. 3A, a and b, lane 2). It was also noted that there may be cross talk between Akt and Src kinases because the Src inhibitor PP1 blocked phosphorylation on Akt motifs and LY294002 blocked phosphotyrosine phosphorylation. The densitometric scan of the blot indicated the significance of the inhibition by PP1 and LY294002. Insulin is known to activate Src in skeletal muscle (31). Hence, Clk/Sty was a substrate for Akt *in vivo*, and insulin coordinated both serine and tyrosine phosphorylation of Clk/Sty.

Because the Clk antibody in Fig. 3A immunoprecipitated both endogenous Clk/Sty as well as overexpressed Clk, we then examined whether endogenous Clk/Sty was phosphorylated on its Akt substrate motifs in L6 myotubes. Increased phosphorylation of endogenous Clk/Sty immunoprecipitates was detected by the Akt substrate antibody, and phosphorylation was blocked by LY294002 (Fig. 3B, a). The IgG band was evident because a polyclonal antibody was used. It is evident that Clk/Sty was a substrate for insulin-activated Akt signaling in both transfected COS7 cells and in cultured L6 myotubes.

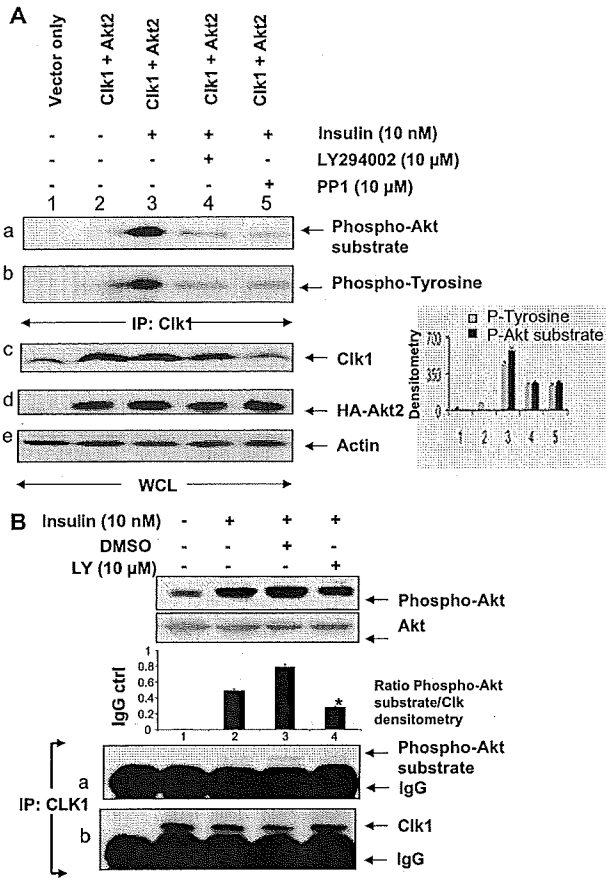

FIG. 3. Akt2 involvement in Clk/Sty activation and Clk/Sty-mediated SR protein phosphorylation. A, Transiently expressed Clk/Sty was phosphorylated by Akt2. COS7 cells were transiently transfected with Clk/Sty, Akt2, or pcDNA3 control vector constructs for 36 h with Lipofectamine. After serum starvation for 6 h, cells were stimulated by insulin (10 nM, 30 min), and whole-cell lysates were immunoprecipitated with anti-Clk/Sty (IP: Clk1). The phosphorylation of tyrosine residues and Akt-substrate serine residues on Clk/Sty was analyzed by Western blot using anti-phosphotyrosine or anti-phospho-Akt substrate antibodies (*top panels* a and b). Whole-cell lysates run on gels were probed for Clk1, Ha-Akt2, and actin (*lower panels* c, d, and e). The graph to the *right* shows a densitometric scan of the Clk1 IP probed with anti-phospho-Akt substrate (*black bars*) and anti phosphotyrosine (*gray bars*). (For this and subsequent figures, the *P* value was determined using a two-tailed unpaired Student's *t* test.) Lanes 4 and 5 were significantly ($P < 0.005$; n = 3) inhibited compared with lane 3. This experiment was repeated on three occasions with similar results. B, Endogenous Clk/Sty was phosphorylated by Akt2 during insulin signaling. L6 myotubes were serum starved, insulin stimulated, and lysed (WCL); Clk/Sty was immunoprecipitated and analyzed for phosphorylation of Akt-substrate serine residues as above (*lower panels*). Due to the difference in antibody source (polyclonal *vs.* HA-tagged), IgG is detected. The graph *above* the blot represents the densitometric scans for Clk1 IP probed with phospho-Akt substrate antibody. Inhibition of Clk phosphorylation in lane 4 was significant ($P < 0.005$; n = 3) compared with lane 3. Phosphorylation of Akt induced by insulin was confirmed with phospho-Akt-473 antibody (*top panel*).

SR proteins as Clk/Sty substrates

We hypothesized that both Akt2 and Clk/Sty participated in the phosphorylation of SR splicing factors. To determine whether insulin-activated Akt2 modulated Clk/Sty-mediated SR protein phosphorylation, we examined the effects of Clk/Sty- and Akt2-specific siRNA on SR protein phosphorylation (Fig. 4). Because insulin increased the intensity of phosphorylated SR proteins when detected with mAb104, we reasoned that the motif recognized by this antibody, Arg/Ser-rich regions, would be specific to Clk/Sty and Akt2. Clk/Sty- and Akt2-specific siRNA suppressed protein levels of Clk/Sty or Akt2, respectively, in transfected L6 myotubes (*top panels* a–c using whole-cell lysates). SRp75, SRp55, and SRp30b/SC35, identified previously as substrates for insulin-induced phosphorylation (15), were immunoprecipitated from L6 cell lysates after insulin stimulation and then separated by SDS-PAGE. Clk/Sty- or Akt2-specific siRNA-induced depletion (series 1 siRNA shown and data from series 2 not shown but corroborating results) markedly suppressed insulin-induced phosphorylation of SRp75, SRp55, and, to a lesser extent, SRp30b/SC35 (Fig. 4, d, f, and h). The identities of these SR proteins were confirmed by reprobing the same membranes with the corresponding SR protein antibodies, namely SRp75, SRp55, and SRp30b/SC35 (Fig. 4, e, g, and i). These results indicated that both Akt2 and Clk/Sty participate in SR protein phosphorylation. Because pre-mRNA splicing of PKCβII was also altered by Akt2 and Clk/Sty as shown earlier (Figs. 1 and 2), SR protein phosphorylation is likely to be the next step in the Akt2/Clk cascade.

Akt2 modulates Clk/Sty-mediated SR protein phosphorylation

Akt2 phosphorylated Clk/Sty, and it activated Clk/Sty-mediated SR protein phosphorylation and βII exon inclusion in response to insulin stimulation (Figs. 1, 3, and 4). To distinguish between the effects of PI3K/Akt2 on Clk/Sty activation and SR protein phosphorylation, a Clk inhibitor was used. Clk/Sty and Akt2 were cotransfected into L6 myotubes and the cells treated with DMSO, a control, a PI3K inhibitor (LY294002), the Clk inhibitor (TG003) (28), or its control compound, TG009, before insulin stimulation. Akt2 rather than the constitutively active Akt2 was used so that insulin activation of phosphorylation could be demonstrated. Both HA-tagged Akt2 and HA-tagged Clk/Sty were overexpressed at detectable levels, demonstrated by anti-HA, anti-Akt, and anti-Clk/Sty immunoblotting (Fig. 5, g–i). Insulin induced the phosphorylation of Akt in transfected L6 myotubes (Fig. 5j) and serine phosphorylation was blocked by the PI3K inhibitor LY294002 (Fig. 5j, lane 15). The role of Akt2 in promoting phosphorylation that was detected by mAb104 antibody here was likely mediated through Clk, although other kinases cannot be ruled out.

Phosphorylation of ERK1/2 (a MAPK pathway also activated by insulin) was similarly induced by insulin, but its phosphorylation was not affected by either the Clk inhibitor TG003 or the PI3K inhibitor LY294002 (Fig. 5k), confirming that both inhibitors were specific for their target kinases. TG009, a control compound for TG003, had no effect (Fig. 5, a, c, and e, lanes 12–13). Importantly, when transfected alone, both Akt2 and Clk/Sty increased the serine phosphorylation of SRp75 and SRp55 (Fig. 5, a and c, lanes 3 and 5), as detected by mAb104, which recognizes phosphoserines in Arg/Ser regions.

Clk/Sty appears to be the stronger kinase, enhancing serine phosphorylation, because a marked reduction in phosphorylation occurred in the presence of its specific inhibitor. Cotransfection of Clk/Sty and Akt2 increased the serine phosphorylation of SRp75 and SRp55, which was suppressed best by TG003 (Fig. 5, a and c, lanes 10–11). The inhibition of phosphorylation was

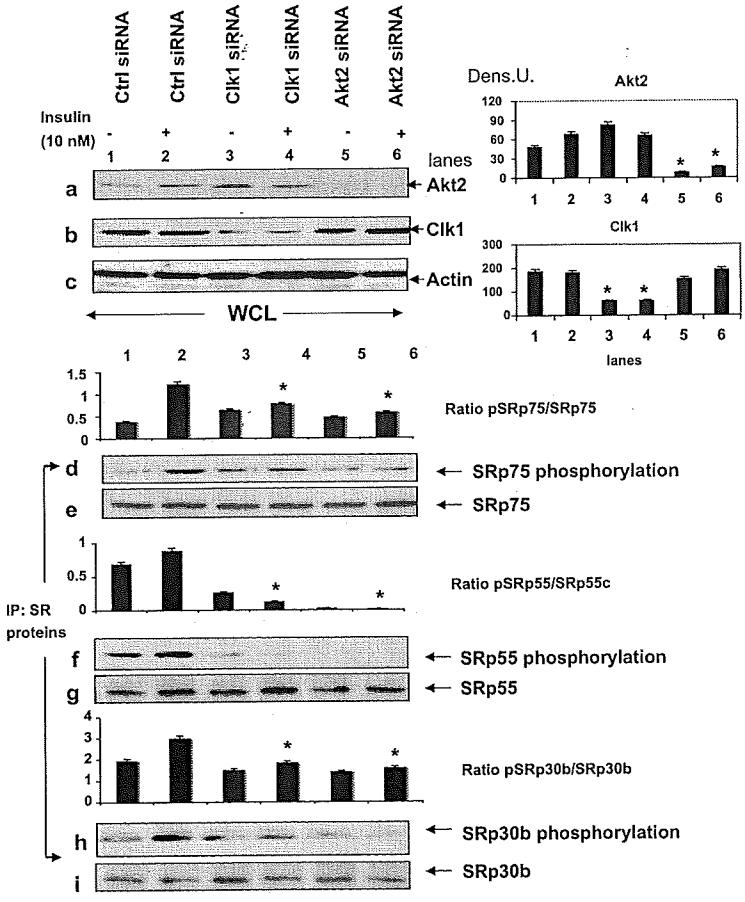

FIG. 4. Akt2 and Clk/Sty siRNA suppress insulin-induced SR protein phosphorylation on RS domains. L6 cells were transfected with Clk/Sty, Akt2, or control (Ctrl) siRNA for 48 h as indicated in Fig. 2 (series 1), serum starved (6 h), insulin stimulated, and then lysed. Effectiveness of the siRNA was examined on protein levels with anti-Clk/Sty and anti-Akt2 (*top panels*). The graphs to the *right* are densitometric scans of the blots indicated and demonstrate significant ($P < 0.05$) reduction of Akt2 and Clk1 by the appropriate siRNA. SR proteins were individually immunoprecipitated and immunoprecipitates (IP: SR proteins) examined for phosphorylation of RS domains by mAb104 (*lower panels*). The identities of SR proteins in the immunoprecipitates were confirmed by stripping the blot and reprobing with appropriate SR protein antibodies. Graphs represent phospho-SR/SR protein (pSRp/SRp) ratio specified. The experiment was repeated twice. The inhibition of SR protein phosphorylation by Clk1 siRNA and Akt2 siRNA was significant ($P < 0.05$) for each SR protein compared with the insulin-stimulated sample (lane 2). A second set of siRNA to Clk/Sty and Akt2 also blocked SR protein phosphorylation (data not shown). Dens. U, Arbitrary densitometry unit.

less dramatic with LY294002 (Fig. 5, a and c, lane 14) but significant in the presence of insulin ($P < 0.05$) (Fig. 5, a and c, lane 15). Increases in phosphorylation induced by Akt2 or Clk/Sty in SRp30b/SC35 were less dramatic (Fig. 5e), and the sensitivities to PI3K and Clk/Sty inhibitors were much weaker compared with that found for SRp75 and SRp55, indicating that SRp30b/SC35 was not a preferred substrate in the insulin pathway. Clk/Sty regulation induced by Akt2 (Fig. 5, a and c) is consistent with the data shown in Fig. 4 using Clk/Sty and Akt2 siRNA to specifically reduce protein levels. In addition, inhibition of SR protein phosphorylation by the PI3K inhibitor LY294002 was not as dramatic as that of the Clk inhibitor TG003 (Fig. 5, a and c), suggesting that there may be a basal activity of Clk/Sty or an alternate cascade for Clk/Sty activation. However, our data clearly indicate that Akt2 and Clk/Sty are both required for full insulin-induced phosphorylation of SRp75 and SRp55, and when viewed with the splicing data in Figs. 1B and 3, Clk/Sty appeared to be acting downstream of PI3K/Akt2 in modulating SR protein phosphorylation. These studies demonstrated that insulin also regulated SRp75 and SRp55 phosphorylation via Clk/Sty signaling.

PI3K/Akt2 regulates serum-induced, Clk/Sty-mediated SR protein phosphorylation

Insulin regulation of splicing is best demonstrated after serum starvation. As shown so far (Figs. 1–5), PKCβII exon inclusion in response to insulin stimulation was blocked by the Clk/Sty inhibitor and its siRNA, and by knocking down and inhibiting Akt2, a potential activator of Clk/Sty. The SR protein targets of Clk/Sty identified here were SRp75, SRp55, and SRp30b. To ascertain whether Akt2 and Clk/Sty regulation of phosphorylation and resulting activation of SR splicing factors was specific to insulin or represented a universal phenomenon, we examined whether SR proteins were substrates for Akt2-regulated Clk/Sty activation under culture conditions in the presence of 10% fetal calf serum, conditions that promote cell growth.

Clk/Sty and Akt2 were transfected into differentiated L6 cells before treatment with LY294002 or TG003 (32). In this case, we examined SRp75 and SRp30b. The cotransfection increased the serine phosphorylation of SRp75 as detected by mAb104 (Fig. 6a, lanes 4 and 5), and this was blocked by TG003 and LY294002 (lanes 6 and 8). The control, TG009, also had an inhibitory effect but was not as great as TG003 (Fig. 6a, lane 7). The possibility that TG009 may inhibit Akt or another upstream kinase under serum conditions was a possibility (Fig. 6e, lane 7). With serum present, SRp30b/SC35 appeared to be phosphorylated in a Clk/Sty- and Akt2-dependent manner with respect to TG003- and LY294002-mediated inhibition (Fig. 6c). Simultaneous analysis of Akt phosphorylation demonstrated an inhibition by LY294002 but no alteration by TG003 (Fig. 6e, lane 6). Importantly, cotransfected Akt2 enhanced Clk/Sty-mediated SRp75 phosphorylation, which was only partially blocked by LY294002, and especially by TG003, and demonstrated a requirement for Akt2 in Clk/Sty activation (Fig. 6a, lane 2 *vs.* 4, 6, and 8). Akt2 and Clk/Sty transfection caused no changes in SR protein levels (Fig. 6, b and d). Control blots for Akt2, Clk/Sty, HA, and actin supported the changes observed on protein phosphorylation and indicated that Clk/Sty was endogenously expressed in L6 cells (Fig. 6, f, h, and i). Hence, Akt2 enhanced the action of Clk/Sty on SRp75, suggesting a PI3K/Akt2→Clk/Sty connection was involved in the regulation of SRp75 phosphorylation induced by serum. These data demonstrated a requirement for PI3K/Akt2 in Clk/Sty phosphorylation of SRp75 and SRp30b/SC35 in response to serum. Compared with insulin, serum induced a much

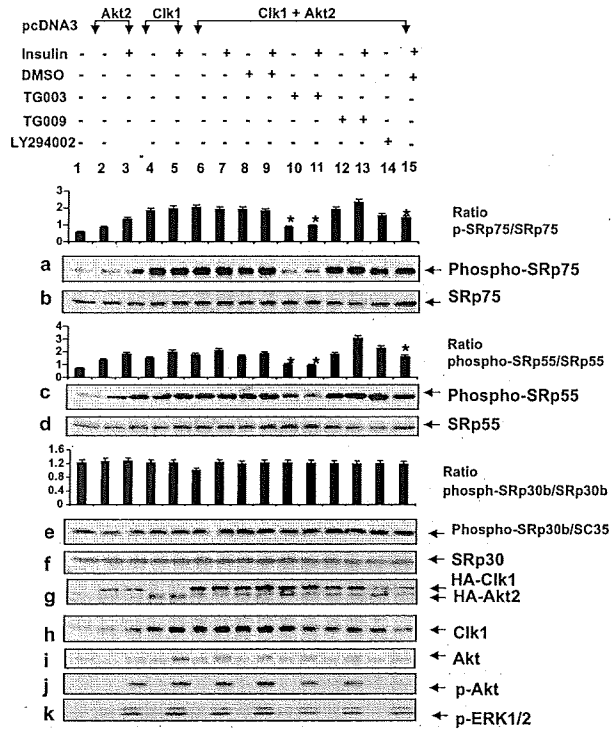

FIG. 5. Akt2 regulates Clk/Sty-mediated SR protein phosphorylation in insulin signaling. L6 myotubes were transfected with pcDNA3 vector, Akt2, Clk/Sty, or Akt2 plus Clk/Sty constructs as indicated for 36 h, serum starved for 6 h, and then treated with Clk/Sty-specific inhibitor TG003 (10 μM) or control compound TG009, LY294002 (10 μM), or DMSO for 60 min before insulin stimulation (10 nM, 30 min), lysed, and analyzed for SR protein phosphorylation with mAb104 in addition to evaluation of the expression of the transfected genes (g), phospho-Akt (p-Akt) and phospho-ERK1/2 (p-ERK1/2; j and k). Identities of the SR proteins were confirmed by reprobing the stripped blots with the appropriate antibodies. The graph *above* each SR protein is the ratio of phospho-SR/SR protein (p-SRp/SRp). *, Inhibition of phosphorylation by TG003 or LY294992 is significant ($P < 0.05$; n = 3) using a two-tailed unpaired *t* test compared with lanes 7 and 9 with insulin.

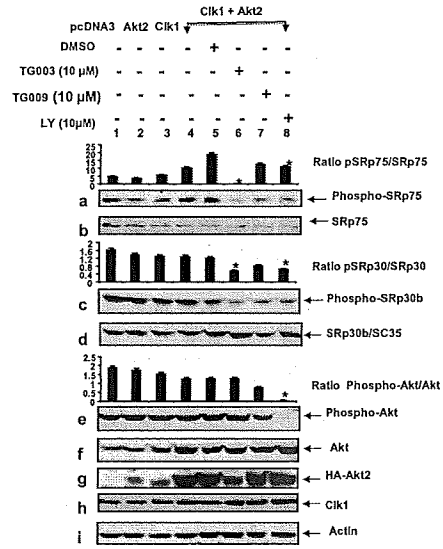

FIG. 6. Akt2 regulates SR phosphorylation both by itself and by stimulating Clk/Sty-mediated action in response to serum and insulin. L6 myotubes were transfected with pcDNA3 vector, Akt2, Clk/Sty plasmids, or Akt2 plus Clk/Sty plasmids as indicated for 36 h in 10% serum and treated with TG003, LY294002 (LY; 10 μM), or DMSO for 60 min. Cells were then lysed and analyzed with mAb104 by Western blot. Cell lysates were also evaluated for expression of transfected genes, phospho-Akt, SR protein levels, and β-actin. Specific SR proteins were identified by reprobing the blots with antisera after stripping mAb104 as indicated. The graphs are the ratio of the phosphorylated protein/protein for SRp75 (pSRp75/SRp75), SRp30b (pSRp30/SRp30), and phospho-Akt. *, Significant ($P < 0.05$; n = 3) inhibition of phosphorylation compared with the control lane 5.

stronger phosphorylation on SRp30b/SC35 (Figs. 5e and 6c) because TG003 did not block insulin phosphorylation of SRp30b in Fig. 5e (lanes 10–11), suggesting that this serum-initiated, Akt2-mediated Clk/Sty pathway was distinct from the one stimulated by insulin, *i.e.* insulin and serum induce phosphorylation of different SR proteins. Thus, SRp30b/SC35 appears not to be a preferred substrate for Clk/Sty during insulin stimulation.

SR proteins as direct substrates for Akt2

SR proteins have considerably more Akt phosphorylation motifs than Clk/Sty phosphorylation motifs. These motifs are all within the Arg/Ser domains. Thus, the potential for Akt2 to directly phosphorylate SR proteins on multiple sites is high. We examined Akt2-mediated phosphorylation of SR proteins in response to insulin stimulation, using an antibody for the phosphorylated Akt substrate motif. The antibody provides data similar to that of the conventional *in vitro* kinase assays for Akt2 as demonstrated by the effects of insulin on SRp40 phosphorylation (5). The antibody technique may even be preferable, because *in vitro* kinase assays cannot rule out the possibility of interacting kinases as we have described here. Insulin- and serum-stimulated serine phosphorylation on Akt-substrate motifs in SRp75 and SRp30b/SC35 (Fig. 7, c and e). Inhibition of PI3K/Akt signaling blocked this phosphorylation (lane 5); Src kinase inhibitor PP1 also reduced the intensity of phosphorylation, suggesting that there was further fine tuning of SR protein phosphorylation by Src family members (Fig. 7, c and e, lane 4). The results indicated that these SR proteins were also directly controlled by Akt2, as had been suggested by previous reports (5, 21, 33).

Because both Akt2 and Clk/Sty could phosphorylate the same Serine residues within Arg/Ser domains, and because there are more Akt substrate motifs than Clk/Sty motifs in SR proteins, we hypothesized that SR proteins phosphorylated by Akt2 should display different phosphorylation patterns from those effected by Clk/Sty. We examined the differences in phosphorylation patterns caused by inhibition of PI3K/Akt only or Clk/Sty only. For this purpose, we reprobed the same membranes described in Fig. 5 with phosphorylated Akt substrate antibody. The phosphorylation patterns revealed with the phospho-Akt substrate antibody were quite different from those revealed by mAb104, a widely used monoclonal antibody in SR protein studies, which appeared to detect predominately Clk/Sty-mediated phosphorylation (Fig. 5, a, c, and e, and Fig. 8, a, c, and e), indicating that Akt2 and Clk/Sty are working on different serine residues within the same Arg/Ser domains of SR proteins. For example, SRp30b/SC35, which was not significantly impacted by the Clk/Sty inhibitor (Fig. 5e), had a dramatically different insulin-dependent phosphorylation pattern that was blocked by the Akt signaling

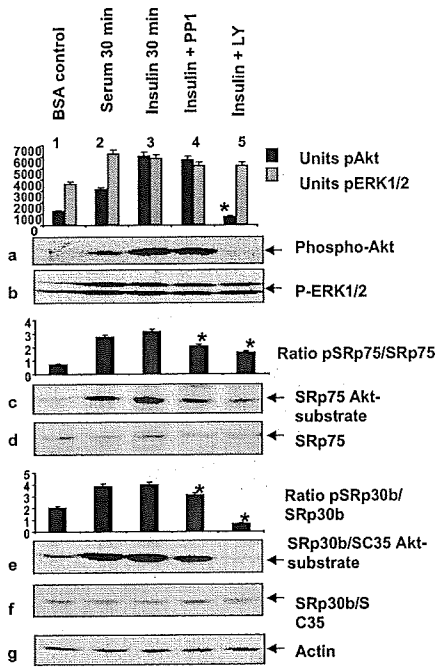

FIG. 7. Akt2 phosphorylates SR proteins in response to insulin and serum. L6 myotubes were serum starved, pretreated with 10 μM LY294002 or tyrosine kinase inhibitor PP1 for 60 min, and then stimulated with serum or insulin for 30 min. The cells were lysed and analyzed for Akt-mediated phosphorylation of SR proteins, Akt and ERK1/2 phosphorylation by Western blot similar to what was described in Fig. 6. The densitometric scan is plotted as a bar graph for units of phospho-Akt (pAkt) and phospho-ERK1/2 (P-ERK1/2). The inhibition by phospho-Akt by LY294992 is significant ($P < 0.05$) compared with the insulin-stimulated sample. Specific SR proteins were identified by reprobing the blots after mAb104 with antisera as indicated. Graphs for SRp75 and SRp55 represent ratios of phosphorylated SR protein/SR protein. The inhibition by LY294002 is significant ($P < 0.05$; n = 3) as determined by a two-tailed unpaired *t* test. β-Actin was detected as an internal control.

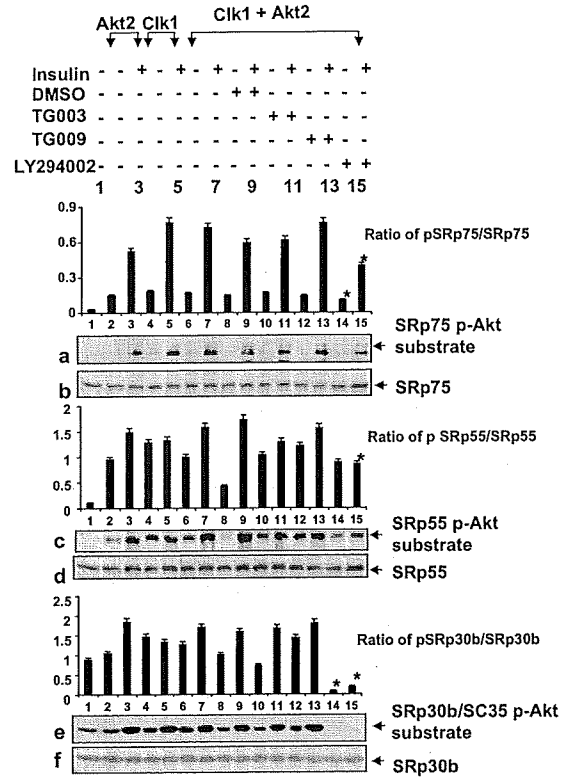

FIG. 8. Akt2 phosphorylates SRp75, SRp55, and SRp30b in Clk1- and Akt2-transfected cells. L6 myotubes were transfected with pcDNA3, Akt2, Clk/Sty, or Akt2 plus Clk/Sty plasmids as indicated for 36 h, serum starved for 6 h, and then treated with TG003, TG009, LY294002, or DMSO for 30 min before insulin stimulation (10 nM, 30 min; see Fig. 3), lysed, and analyzed for SR protein phosphorylation with phospho-Akt (p-Akt) substrate antibody in addition to evaluation for expression of the transfected genes and Akt phosphorylation by Western blot (shown in Fig. 3). Identities of these SR proteins were confirmed by reprobing the stripped blots with the corresponding antibodies (also shown in Fig. 3). The graphs are ratios of phospho-SR protein/SR protein (pSRp/SRp). *, Inhibition of phosphorylation was significant ($P < 0.05$; n = 3).

inhibitor LY294002 (Fig. 8e, lanes 14–15). These data suggest that SRp30b/SC35 is a preferred Akt2, but not Clk/Sty, substrate in insulin signaling and that Akt2 phosphorylates SR proteins directly in addition to Clk/Sty. The partial inhibition of SRp75 phosphorylation by LY294002 also suggests that another kinase may be phosphorylating some of the serine sites. The results implicated both Akt2 and Clk/Sty in the control of SR proteins and further suggested that the actions of Akt2 and Clk/Sty were distinctly different on each protein.

Akt2 is linked to Clk/Sty regulation *in vivo*

Clk/Sty kinases may be linked to the genetic susceptibility to type 2 diabetes in mice (34). To verify that the activation pathway observed in differentiated L6 cultures was related to that in the intact animal, we examined Clk/Sty phosphorylation on phospho-Akt substrate sites in tissues obtained from Akt2-null mice with insulin resistance and from wild-type mice (25). Tissues from skeletal muscle and liver were homogenized, Clk/Sty protein was immunoprecipitated, and the immunoprecipitates were analyzed by immunoblot using phosphorylated Akt substrate antibody or anti-Clk (Fig. 9). Samples from each of four Akt2-null mice had substantially decreased phosphorylation of Akt-substrate sites in Clk/Sty, compared with samples from two wild-type mice, indicating that Akt2 mediated the phosphorylation of Clk/Sty in the wild-type pathway and that absence of Akt2 led to reduced phosphorylation of Clk/Sty. The animal study further corroborated our observation that Akt2 is an upstream regulator of Clk/Sty *in vivo*.

Akt2 participated in maintaining normal phosphorylation of SRp55 and PKCβII levels

Western blot analysis of brain, muscle, and liver tissue lysates from Akt2-null mice showed that Akt phosphorylation of SRp55 was dramatically decreased in tissues from the null mice compared with wild-type mice (Fig. 9). The decrease in Akt phosphorylation/activation, we believe, was due to the absence of Akt2 protein, but the presence of Akt1 and Akt3 (Fig. 9a). All three phospho-Akt isoforms are recognized by the Akt-substrate antibody. Nevertheless, analysis of SRp55 from the Akt2-null mice revealed a corresponding and significant suppression of phosphorylation, compared with wild-type mice (Fig. 9b). SRp55 was the SR protein with the most dramatic decrease in phosphorylation with Clk siRNA; hence, it was thought to best represent Clk effects on the RS domain. Previously, we showed that PKCβII

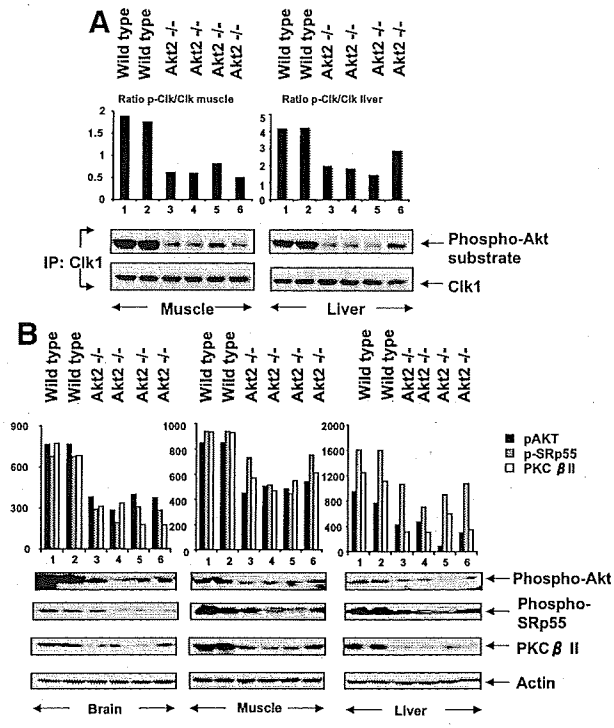

FIG. 9. Reduced PKCβII expression and impaired Clk/Sty and SRp55 phosphorylation in Akt2-null mouse tissue. A, Impaired Clk/Sty phosphorylation in Akt2-null mouse tissues. Gastrocnemius and liver tissue samples were obtained from wild-type and Akt2-null mice. Tissue homogenates were immunoprecipitated with anti-Clk/Sty, and immunoprecipitates after SDS-PAGE were probed with Clk/Sty and phospho-Akt (p-Akt) substrate antibody. The graph of densitometric scans is a ratio of phospho-Clk (p-Clk)/Clk. For muscle, the wild-type ratio is 1.82 ± 0.06 (n = 2) and for Akt2$^{-/-}$ 0.62 ± 0.06 (n = 4); $P < 0.003$. For liver, the wild-type ratio was 4.18 ± 0.02 (n = 2) and for Akt2$^{-/-}$ 2.05 ± 0.28 (n = 4); $P < 0.007$. B, Impaired SRp55 phosphorylation and suppressed PKCβII expression in Akt2-null mouse tissues. Brain, gastrocnemius, and liver tissue samples after SDS-PAGE were analyzed for Akt phosphorylation at serine 473, phosphorylation of SRp55 recognized by mAb104, PKCβII, and actin levels. The graph *above* each tissue blot is the densitometric scan for the phosphorylated protein identified on the *right*. In each case, the phosphorylation or protein level was lower in the tissue from the Akt2$^{-/-}$ tissue compared with the wild type as summarized in Table 1.

mRNA levels, but not PKCβI mRNA, were decreased in these animals (5); the Western blot analysis revealed that PKCβII protein levels were dramatically decreased (>75%) in Akt2-null mice (Fig. 9B), which demonstrated a functional requirement for Akt2 and Clk/Sty in the expression of PKCβII. The statistical analysis of densitometric scans of phospho-Akt, phospho-SRp55, and PKCβII from Fig. 9 and presented in Table 1 indicated that the Akt2$^{-/-}$ tissues contained significantly lower levels of phosphoproteins compared with corresponding wild-type tissues.

TG003 blocked insulin-stimulated glucose uptake

The importance of PKCβII for insulin-stimulated glucose uptake in L6 cells was previously demonstrated (19). To test whether Clk/Sty mediated this, we preincubated L6 cells with TG003 for 2 h before insulin treatment (30 min) and 2-deoxyglucose uptake. In Fig. 10, the Clk inhibitor TG003 significantly blocked insulin effects of glucose uptake under these treatment conditions.

TABLE 1. Statistical analysis of densitometric scans for wild-type and Akt2$^{-/-}$ tissue Western blots in Fig. 9

Immunoblots	Wild type (n = 2)	Akt2$^{-/-}$ (n = 4)	*P* value
Brain			
pAkt	765 ± 0.5	357 ± 26	0.0005
pSRp55	675 ± .5	267 ± 25	0.0005
PKCβII	727 ± 45	251 ± 42	0.002
Muscle			
pAkt	846 ± 0.5	493 ± 18	0.0002
pSRp55	936 ± 0.5	610 ± 76	0.047
PKCβII	930 ± 0.05	547 ± 30	0.001
Liver			
pAKT	867 ± 90	330 ± 87	0.02
pSRp55	1606 ± 1	938 ± 86	0.007
PKCβII	1192 ± 60	398 ± 69	0.002

Western immunoblots shown in Fig. 9B were scanned as JPEG files, and areas of interest were digitized using UN-SCAN-IT gel digitizing software by Silk Scientific. Densitometric values were imported into Excel (Microsoft Office 2004) and plotted. The values (arbitrary densitometric units) were then analyzed for significance using an unpaired *t* test (Prism4 version 4.0a; GraphPad Software). pAKT, phospho-Akt.

Discussion

Clk/Sty is a dual-specificity kinase shown to phosphorylate SR protein splicing factors predominately on serine residues (7, 8, 11–13, 35). Because Clk/Sty phosphorylation of SR proteins subsequently alters their activity, subcellular localization, and ubiquitination (11–13), we sought to understand the mechanism by which Clk/Sty itself is regulated. Analysis of Clk/Sty protein revealed prominent phosphorylation on both serine/threonine and tyrosine residues (7), leading us to question whether it was regulated by any other serine/threonine kinase in addition to autophosphorylation. In this study, we determined Clk/Sty was regulated by a PI3K/Akt2 kinase pathway *in vivo* based on a number of criteria.

First we determined that Akt2 and Clk/Sty kinases were essential for insulin-mediated PKCβII splicing and expression. Our

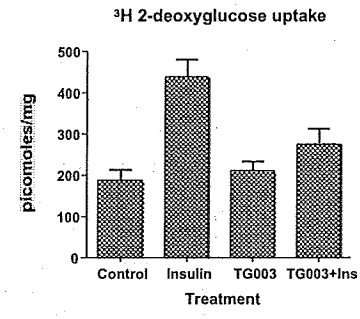

FIG. 10. Inhibition of insulin-stimulated glucose uptake by TG003. L6 myocytes were serum starved for 4 h in Dulbecco's PBS with or without 10 μM TG003 for 2 h. Insulin (50 nM) was added for 30 min before [^{3}H]2-deoxyglucose for 6 min at 37 C. Uptake was stopped by aspirating the media and rinsing cells with ice-cold Dulbecco's PBS. An aliquot of solubilized cell lysate was counted by scintillation counting for cellular uptake. Cytochalasin B-inhibitable counts were determined routinely and found to be less than 25% of control counts per minute. The data (mean ± SEM) are from the averages of four separate experiments performed in triplicate for each point. Data were converted to specific activity and analyzed by Prism4 software using a one-way ANOVA with Tukey's multiple comparison test. Control *vs.* insulin, $P < 0.001$; insulin *vs.* TG003 plus insulin (Ins), $P < 0.005$.